2024

SEASONAL AND SPATIAL VARIATIONS OF THE SEDIMENT TRANSPORT ALONG THE SOUTHERN SHORE OF RHODE ISLAND

Pumee Rojchanaborworn
University of Rhode Island, projchanab@uri.edu

SEASONAL AND SPATIAL VARIATIONS OF THE SEDIMENT TRANSPORT ALONG THE SOUTHERN SHORE OF RHODE ISLAND

BY

PUMEE ROJCHANABORWORN

A THESIS SUBMITTED IN PARTIAL FULFILLMENT OF THE REQUIREMENTS

FOR THE DEGREE OF

MASTER OF SCIENCE

IN

OCEAN ENGINEERING

UNIVERSITY OF RHODE ISLAND

2024

MASTER OF SCIENCE

THESIS OF

PUMEE ROJCHANABORWORN

APPROVED:

Thesis Committee:

Major Professor: M. Reza Hashemi

Jason Dahl

Tetsu Hara

Malcolm Spaulding

Brenton DeBoef

DEAN OF THE GRADUATE SCHOOL

UNIVERSITY OF RHODE ISLAND

2024

ABSTRACT

This study investigates sediment transport trends in southern Rhode Island by analyzing seasonal and spatial variations in different wave climates using numerical models, specifically XBeach and Simulating Waves Nearshore (SWAN). SWAN simulates offshore wave propagation, while XBeach simulates beach morphology and sediment transport. In terms of temporal variability, this study focuses on Green Hill Beach, Rhode Island, and simulates four seasonal storm conditions, including Hurricane Sandy, Hurricane Irene, nor'easter in the Spring of 2013, and nor'easter in the Fall of 2012. The data from the US Army Corp of Engineers, Northeast Coast Comprehensive Study (NACCS) were also incorporated to examine spatial variations of storms along the southern shore of Rhode Island at each barrier system from Green Hill Beach to Misquamicut State Beach. Nested SWAN models covering a large area of the northeastern US (parent domain) and Rhode Island local waters (child model) were first validated using observed data. The wave modeling study demonstrated that a parametric hurricane model achieves the best results for the large domain. It was also shown that the spatial variability of waves in Rhode Island's local waters (child model) is small enough that a local model can be forced by a uniform wave height. The XBeach model was then nested inside the SWAN child model. XBeach simulations, based on storms like Hurricane Irene, Hurricane Sandy, and the nor'easter of spring 2013, reveal consistent sediment deposition east of Green Hill Beach and variations in sediment erosion on the west. Hurricane Irene (summer) and the 2013 nor'easter (spring) simulations exhibit similar trends, indicating similar sediment transport patterns for winter and summer storms, although with different intensities. This can be justified as sediment transport is

dominated by wave and storm surge impacts, and extreme events can happen during both summer and winter periods. The NACCS dataset highlights spatial variability in wave heights during the 100-year return period event, with a mean of 4.04 m and an 18.32% relative standard deviation across all save points from each beach on the southern Rhode Island coast. East Beach has the largest exposure to wave height (4.99 m), while Point Judith has the lowest exposure (3.0 m). The maximum water level generated by the NACCS 100-year return period water level exhibits slight variation along the south coast with a mean of 2.67 m and a 5.06% relative standard deviation. Only one sediment grain size was considered in the model, and all simulations were run using one consistent bathymetry. A more accurate approach would involve collecting the bathymetry data immediately before and after the hurricane's event and measuring different grain sizes along the southern shore of Rhode Island.

ACKNOWLEDGMENTS

I would like to extend my deepest gratitude to Professor M. Reza Hashemi for all the support, guidance, and mentorship throughout the process and for taking a chance on me. Your influence has been profound, and I am very grateful to have worked with you on designing work for Green Hill beach dunes and this project. I would also like to thank my committee members, Professor Jason Dahl, Professor Tetsu Hara, and Professor Malcolm Spaulding. Your collective wisdom and guidance have been instrumental in shaping my academic journey. Thank you, Professor Dahl, for all your time and dedication. Thank you, Professor Hara, for introducing me to wave and storm surge modeling. Thank you, Professor Spaulding, for all his expert insight on coastal erosion. I would also like to mention special thanks to Jacob Fontaine, Arash Rafiee Dehkharghani, Jensen McTighe, and Megan Gimple for all their support throughout the past two years. Your friendship and support have been invaluable. Additional gratitude toward Zachary Rinchiuso for his time and expertise. Also, special thanks to Brett Ruben and Dr. Leonard Kahn from the physics department. And finally, I'm grateful for everyone I have met at GSO. Every single person has affected my life in one way or another.

Table of Contents

List of Figures

List of Tables

List of Acronyms

ADCIRC	Advanced Circulation Model
CDIP	The Coastal Data Information Program
CERC	The Coastal Engineering Research Center
CGEM	Coastal Geomorphic Erosion Model
ECMWF	The European Centre for Medium-Range Weather Forecasts4
GEBCO	The General Bathymetric Chart of the Oceans
JONSWAP	The Joint North Sea Wave Project
LiDAR	Light Detection and Ranging
NACCS	The North Atlantic Coast Comprehensive Study
NCEI	The National Centers for Environmental Information
NOAA	The National Oceanic and Atmospheric Administration
RSM	The Regional Sediment Management
SWAN	Simulating Waves Nearshore
WIS	Wave Information Studies

1. Chapter I. Introduction

1.1. Background

Nearly a quarter of the world's sandy beaches have been eroded due to climatic changes and rising sea levels (Athanasiou et al., 2020). The National Oceanic and Atmospheric Administration (NOAA) has estimated that the sea level could rise between 0.5 and 7 feet by 2100 (NOAA, 2023). The combination of accelerating sea level rise and frequent extreme storms puts approximately one-third of the global coastline at risk of shoreline recession (Luijendijk et al., 2018).

Locally this trend will have an impact on 35% of one- and two-story structures in Matunuck, Rhode Island (Small et al., 2016). Over the years, datasets spanning from 1960 to 2010 have revealed a significant spatial and temporal variability in the shoreline change in southern Rhode Island based on time series of beach profile data (Vinhateiro, 2012). Shoreline mapping has also indicated spatial variability in shoreline recession through five multi-decadal times from 1939, 1951, 1961, 2012, and 2014 in Rhode Island (Boothroyd et al., 2016). The Southern Rhode Island shorelines retreat up to 1.15 m per year (Boothroyd et al., 2016). This recession can adversely affect local communities, impacting the tourism industry and coastal infrastructure.

Understanding the response of beaches to storms is crucial for effectively planning coastal protection projects (Toimil et al., 2017). The dune and beach's reaction to storms can be classified into four distinct regimes according to the Wave-Surge dune interaction processes (D'Alessandro et al., 2022). The first regime, the Swash Regime,

involves waves primarily impacting the foreshore of the dune. In the second regime, the Collision Regime, waves actively erode the base of the dune and transport sediment offshore. In the third regime, the Overwash Regime, waves and storm surges overtop the dune, resulting in the deposition of sediment inland. Finally, the fourth regime, the Inundation Regime, sees waves and storm surges completely eroding and flattening the dune (see Figure 1) (D'Alessandro et al., 2022). Each regime represents a distinct phase in the dynamic interaction between waves and dunes, highlighting the varied processes that shape coastal landscapes. Notably, the Overwash and Inundation Regime highlights the heightened severity of beach erosion resulting from storm surges. Elevated water levels near the shore, caused by storm surges, lead to waves breaking closer to the coastline. Sediment transport occurs within these regimes through longshore and cross-shore transport.

The southern shore of Rhode Island exhibits a diverse range of coastal features, including coastal inlets, coastal ponds, and headlands, which are called barrier systems. Most of the sediment supplied to these barrier systems is from offshore since this area does not contain major rivers to supply the sediment (Boothroyd et al., 1985). The barrier system in the south shore of Rhode Island are labeled in Figure 2.

Ocean wave climates influence the location and magnitude of coastal erosion (Slott et al., 2006). Other parameters that affect sediment transport are beach profile, dune profile, sediment grain sizes, bathymetry, storm surge, wind, and tides.

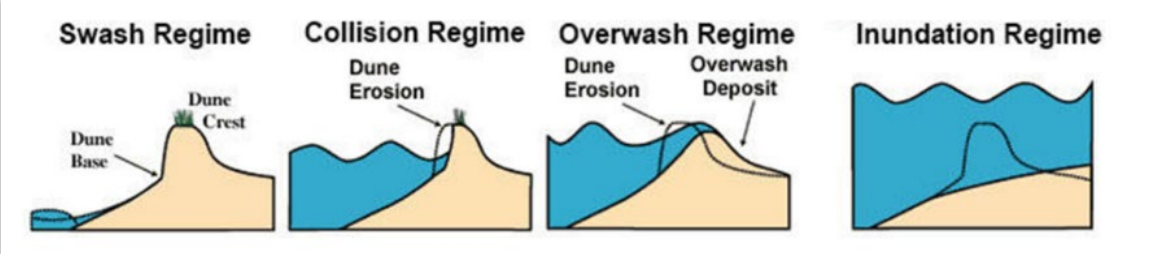

Figure 1. Types of wave-surge dune integration regime (D'Alessandro et al., 2022).

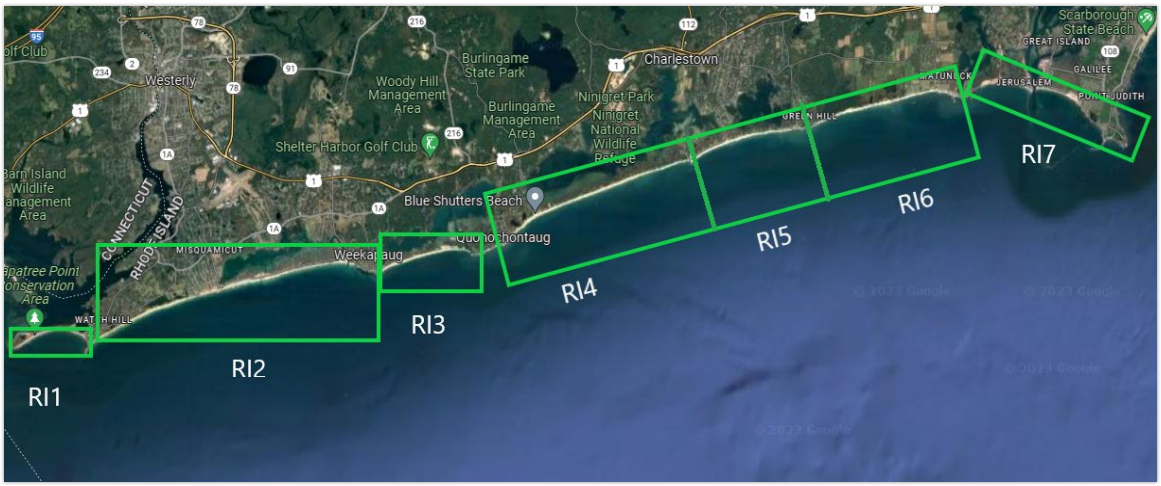

Figure 2. Rhode Island barrier system is labeled by: RI1: Westerly, RI2: Misquamicut (MIS), RI3: Weekapaug (WKG), RI4: East Beach 1 (EB-1), East Beach 2 (EB-2), RI5: Charlestown Beach (CHA-TB), Green Hill (GRH), RI6: Moonstone (MST), RI7: Point Judith

Recognizing the importance of understanding sediment transport for effective coastal protection projects, the U.S. Army Corps of Engineers (2002) emphasizes the importance of estimating the quantity and direction of sediment movement in coastal regions. Traditionally, assessing the movement of sediment along the coast involved visually analyzing satellite images of groins and jetties over a specified time frame (Woods Hole Sea Grant Program, 2021). Numerical modeling techniques such as XBeach and ShorelineS have been increasingly utilized to further understand and predict shoreline changes and beach morphology. For instance, studies by Leone et al. (2022)

and Hayward et al. (2018) have employed these modeling approaches to simulate shoreline changes and assess beach morphology dynamics. The combination of empirical observations, satellite imagery analysis, and numerical modeling techniques provides valuable insights into coastal erosion and sediment transport dynamics, aiding in developing effective coastal management strategies.

A study in California has been conducted using Simulating Waves Nearshore (SWAN) and Coastal Geomorphic Erosion Model (CGEM) by Adams et al. (Adams et al., 2011). They investigated the effect of ocean waves on beach erosion under varying wave directions, using two sets of peak significant wave heights and periods in Southern California Bight (34.58 N, 120.65 W to 32.54 N and 117.12 W). SWAN was used to calculate the shoaling and refraction effects given the input data of wave height, period, direction, and bathymetry. The digital elevation model from NOAA was used as bathymetry input for SWAN. The results, calculated by SWAN, were used as an input into CGEM, which calculated the volumetric transport rates of nearshore sediment. Noted that the CGEM could only be coupled with SWAN stationary mode and is unable to run with data from a time series of changing wave conditions.

The Joint North Sea Wave Project, or JONSWAP, spectrum, with a peak direction of 15 degrees, was used as the wave spectrum in the SWAN stationary mode. The output from SWAN was then imported into CGEM, which used the US Army Corp of Engineers Coastal Engineering Research Center's (CERC) formula to calculate the volumetric sediment transport rate or longshore transport (see Equation 1 below).

$$Q = \frac{I}{(\rho_s - \rho)} g N_0 \quad (1)$$

where ρ_s and ρ are the density of sediment in $\frac{kg}{m^3}$ and seawater $\frac{kg}{m^3}$ respectively, I is the immersed-weight transport rate $\frac{kg*s}{m}$, g is the gravitational acceleration in $\frac{m}{s^2}$, and N_0 is the volume concentration of solid grain. The model was run with two different wave heights, two peak periods, and multiple peak directions ranging from 260 to 320 degrees in 5 increments. The results confirmed that test sites exposed to open sea experienced more transport than the sites with islands in front of them. The paper also indicates that CGEM overestimated the change in sediment volume when sediment supply to the site is limited. Also, the model only considered the sediment transport of the coastal sites, not the rocky beaches along the Southern Californian coast.

A similar method was employed by Ateeth and Jayappa (2020) in Karnataka, India; They used XBeach to simulate waves and sediment transport nearshore and the CERC formula to calculate the longshore transport. The study observed that longshore transport along the coast is affected by wave angle between July and September, indicating seasonal variation in sediment transport. This study merges and refines the methodologies of two previous studies by employing SWAN for wave simulation and XBeach for sediment transport simulation rather than using the formula to calculate the longshore transport. This approach is done to simulate the overall trend of sediment transport using XBeach.

Numerical simulation of coastal erosion and mitigation by living shoreline methods was studied in southern Rhode Island using numerical models like SWAN, ADCIRC (Advanced Circulation Model), and XBeach (Hayward et al., 2018). SWAN and ADCIRC were used to simulate waves and storm surges caused by Hurricane Irene and Hurricane Sandy. SWAN's output wave spectrum and water elevation were used as an input for XBeach which then utilized the data to model the sediment processes and coastal erosions. Areas of study stretched 3 km along Charlestown RI, including Charlestown Breakwater, Charlestown Beach, and Green Hill Beach. The topographic data was taken from NOAA's Montauk location with 1/3 arc second resolution, and the bathymetry data from Northeast Atlantic Vol 2 with 3 arc second resolution. These datasets were interpolated as an input to SWAN. The wind data was taken from the North Atlantic Coast Comprehensive Study (NACCS) as input for ADCIRC. Datasets from the Coastal Data Information Program (CDIP) 175's wave buoy and three transects from the University of Rhode Island's beach profile data were used to validate the results of the SWAN-ADCIRC and the XBeach models, respectively. The SWAN maximum significant wave height was 8.81 m, compared to the observed maximum significant wave height of 9.39 m in the first simulation and 8.59 m compared to the observed value of 9.48 m in the second simulation. These results indicate a mean error of less than 10% for both simulations. The three modeled transects were compared to the different DEM data from 2011 to 2012. The mean value was 17.90 $\frac{m^3}{m}$ and the mean observed value was 21.53 90 $\frac{m^3}{m}$, resulting in a mean error of 23%.

The validated model was then used to analyze the effectiveness of different coastal protection methods, such as living breakwaters, coastal banks, beach nourishment,

and surfing reefs. The result showed that the structures that reinforced the dune were more effective than those that reduced wave action. This study shows the capability of using a numerical model as a research tool for this application. Similar methods of model validation were used in this study.

Another study by Skaden et al. (2021) used XBeach to simulate various storm events with different return periods to determine the effectiveness of reconstructed dunes near Green Hill Pond on the southern shore of Rhode Island. The study used three different models: SWAN, XBeach, and Duna. Duna is a model used to simulate aeolian sediment transport, which is written in Matlab. It requires wind speed data at 10 m elevation and the wind direction normal to the beach profile. It was coupled with XBeach in 1-D to study the beach profile changes. The XBeach boundary condition was forced with 10, 20, 30-year return period storm events. The study stressed the importance of *facua,* a wave skewness and asymmetry parameter in 2-D XBeach and *lsgrad*, a factor used for longshore transport gradient in 1-D XBeach for Duna. The calibration result showed that the best fit *facua* value was 0.35, and *lsglad* was set at 0.0001 in the study. The results indicated that the dunes, designed in Green Hill with an elevation of 4 meters, reduced a significant amount of erosion compared to the unelevated dune. This study will use a *facua* of 0.35 as a starting calibration factor, while *lsglad* will not be utilized since the study is focusing on 2-D XBeach.

Another study by Schambach et al. (2017) on wave and erosion methods for the 100-year storm was done on the southern shore of Rhode Island for five transects around Green Hill Beach. The study used XBeach to simulate sediment transport and NACCS water levels and wave height data as an input to identify various sediment transport

regimes in the study area. Hurricane Irene in August 2011 was used to validate the model's performance. Hurricane Irene simulation was forced by the peak period and peak significant wave height acquired from hindcast data from Wave Information Studies (WIS[1]) station 79. This approach will also be used in this study. Various *facua* parameters ranging from 0.1 to 0.3 were used to calibrate the model. The calibration process showed that increasing the *facua* parameters increased the erosion above the toe of the dune. The study also used various Manning bottom friction factors for each transect. The importance of calibrating the *facua* parameter and using the right Manning bottom friction was demonstrated in this study. The validation results indicate that the collision regime is prevalent throughout the study area. In contrast, the 100-year storm simulation indicated four Inundation regimes and one overwash regime across five transects. Furthermore, Schambach et al. (2018) conducted research on assessing the impact of barrier beaches along the southern coast of Rhode Island, utilizing the same methodology and validation process as mentioned earlier. However, this particular study delves into the effects of friction and vegetation parameters in XBeach. Findings indicated that dune crests' height of 3.6 m lacking vegetation is completely eroded, with sediment transported inland with an overwash regime, whereas vegetated dune crests undergo erosion of 2 meters. The study also underscores the absence of real-time friction adjustment settings in XBeach.

While these studies focused on assessing the impacts of storms on the design of engineering and beach nourishment structures along the southern coast of Rhode Island,

[1] https://wisportal.erdc.dren.mil/

they did not investigate the spatial and temporal variability of beach morphology and sediment transport in the southern coast of Rhode Island.

Understanding the variability of beach morphology and sediment transport is essential for effective mitigation methods. Factors such as wave climate, tide and storm surges, and sediment composition are crucial in shaping the coastline. This study focuses on sediment transport variations by analyzing the influence of wave climate, storm surge, tide, and bathymetry using SWAN and XBeach models. Examining these trends over time provides valuable insights into the evolving nature of the coastal environment. Understanding spatial variability across different beach environments and conditions along the coastline can better inform and tailor the coastal design and structure to fit the diverse environments better. Additionally, insight into seasonal variability allows future coastal design to anticipate challenges and develop adaptive mitigation strategies. Integrating both aspects can enhance the resilience of coastal communities to climate change's impact.

1.2. Research Goal

This research aims to investigate the spatial and temporal variation of sediment transport in the southern coast of Rhode Island, focusing on seasonal and spatial variability of wave climates. Rhode Island is a unique area in that it does not have a major river to supply sediment from inland and consists of multiple headlands separated by each barrier system. Sediment is expected to be trapped between headlands in each barrier system and transported in different directions depending on the wave's angle approaching the shoreline. Additionally, waves and tides are expected to intensify during the storms.

Numerical models such as XBeach and SWAN will be used to simulate the sediment transport and wave propagation respectively. Seasonal variability will be studied by simulating four different storms at Green Hill Beach, Rhode Island, specifically Hurricane Irene during the summer of 2011, Hurricane Sandy during the Fall of 2012, and nor'easters in the Fall of 2012 and Spring of 2013. This approach aims to capture the diverse impact of storms across different seasons on sediment transport. SWAN will be utilized to simulate wave propagation from these storms. The waves propagated by SWAN will serve as boundary conditions for XBeach. XBeach will simulate beach morphology and sediment transport from the wave climate during each storm.

1.3. Thesis Structure

In this study, two numerical models, SWAN and XBeach, are employed with three domains alongside existing data to supplement the research. This study is divided into five chapters: Introduction, Wave Model, Sediment Transport Model, Analysis of Other Available Wave and Morphological Data, and Concluding Remarks. Chapter II: Wave Model will present SWAN's wave simulations and results. SWAN is used in this study to model the wave's climates on the southern coast of Rhode Island, and the resulting waves are used as an input for XBeach to model the beach morphology at RI5: Green Hill (See Figure 2). Chapter III: Sediment Transport Model will covers XBeach models and results; Since storms are the primary driving force of beach morphology, different seasonal storms will be simulated in SWAN then passed on to XBeach in RI5: Green Hill as labeled on Figure 2 to analyze the effect of each storm on the beach. Different storms include Hurricane Irene in the Summer of 2011, Hurricane Sandy in the Fall of 2012, nor'easter in the Winter of 2013, and nor'easter in the spring of 2011.

Additional analysis of wave and morphology data using WIS, the NACCS data, and the Graduate School of Oceanography (GSO) beach profile are conducted in Chapter IV: Analysis of Other Available Wave and Morphological Data. Wave climate data from WIS for each season will also be analyzed for seasonal wave and wind variability. NACCS data will be used to examine the spatial variability of the storms at different save points, and the GSO beach profile will be used to look at variations in beach profiles. The general conclusion and summary will be provided in Chapter V: Concluding Remarks to summarize all the crucial findings

2. Chapter II. Wave Model

2.1. SWAN Introduction

SWAN is a third-generation wave model that simulates ocean waves based on input conditions such as wind, current, bathymetry, and friction (Booij et al., 1999). SWAN uses a wave action balance equation to simulate the wave, see Equation 1.

$$\frac{\partial N}{\partial t} + \nabla_x \cdot \left[\left(\vec{C}g + \vec{u}\right)N\right] + \frac{\partial C_\sigma N}{\partial \sigma} + \frac{\partial C_\theta N}{\partial \theta} = \frac{S_{tot}}{\sigma} \quad (1)$$

The wave balance equation consists of N wave action density ($\frac{E(\sigma,\theta)}{\sigma}$) which is a conserved quantity unlike wave energy density ($E(\sigma,\theta)$) by itself (Whitham, 1974). S_{tot} is the total wave action that includes wave action, white capping, bottom friction, and nonlinear effect. Note that, statistically, wave energy and wave action spectrum are based on both spatial space (x, t) and spectral space (σ, θ), where x is the distance in space, t is time, σ is the wave frequency and, θ is the wave phase direction. All information in wave and sea surfaces is described within this spectrum. The first term shows the changes in wave action density with respect to time t. The second term represents the wave energy propagation in 2-D spatial space, hence the vector notation for C_g group velocity of the wave in $\frac{m}{s}$, $\vec{u}$ velocity of the current. The third and fourth terms represent the flux in frequency σ in radians and direction in θ radians due the changes in depth and mean currents. C_σ and C_θ is the propagation velocity in spectral space. S_{tot} is the non-conservative term which includes all physical processes of wave forms such as wind generation S_{in}, non-linear wave interactions though three-wave (triplet) S_{nl3}, four-wave

interaction (quadruplet) S_{nl4}, bottom friction dissipation $S_{ds,b}$, wave breaking $S_{ds.br}$, and wave decay from white capping $S_{ds,w}$ see Equation 2 (Booij et al., 1999).

$$S_{tot} = S_{in} + S_{nl3} + S_{nl4} + S_{ds,w} + S_{ds,b} + S_{ds,br} \quad (2)$$

The model can simulate several wave processes based on inputs, such as the energy transported by the wave from wind input. Wind generation S_{in} is part of the S_{tot} term. SWAN uses the sum of linear growth terms A by Cavaleri and Malanotte-Rizzoli 1981 and exponential growth B by Komen et al., 1984.

$$S_{in}(\sigma, \theta) = A + B\, E(\,(\sigma, \theta)) \quad (3)$$

where A is

$$A = 0.0015(U_* \cos\,(\theta - \theta_w)^4 H \quad (4)$$

SWAN uses the wind speed at 10 m elevation U_{10} to evaluate for the friction velocity U_* with

$$U_*^2 = C_D U_{10}^2 \quad (5)$$

where C_D, the drag coefficient from Wu (1982) is then expanded using 2nd order Taylor series approximation. The first term of the approximation is 0.00055, while H is the term used to filter frequencies lower than the Pierson-Moskowitz frequency and θ_wIs the wind direction.

The expression of B in terms of wave phase speed C_p, the density of air ρ_a, density of water ρ, and Miles' constant β is as follows.

$$U_*^2 = \beta \frac{\rho_a}{\rho} \left(\frac{U_*}{C_p}\right)^2 (\cos(\theta - \theta_w)^2 \quad (6)$$

The growth term can be calibrated with different β constants. In this case, the model uses the default setting.

2.2. Methods

2.2.1. Wave Modeling Data

In this study, two modes of the SWAN model will be utilized: non-stationary and stationary, with two SWAN domains (parent grid and child grid), respectively. The first (parent) domain is set in the North Atlantic, and the second (child) domain is set in Rhode Island. The next section provides detailed information on these modes and domains. Two types of datasets will be employed: input data and validation data. The input data, which include bathymetry, boundary conditions, and forcing, will be sourced from the General Bathymetric Chart of the Oceans (GEBCO)[2], Coastal Relief Models[3], WIS[4], the European Centre for Medium-Range Weather Forecasts[5] (ECMWF), and parametric wind data (Hashemi et al., 2021). The validation data, used to verify the model's accuracy, will be obtained from the CDIP[6] and the Woods Hole Regional Management (Woods Hole Group, 2012).

GEBCO is a non-profit organization that provides the public with accessible bathymetric information for the Earth's oceans; it functions under the combined auspices

[2] https://www.gebco.net/data_and_products/gridded_ bathymetry_data/
[3] https://www.ncei.noaa.gov/products/coastal-relief-model
[4] https://wisportal.erdc.dren.mil/
[5] https://www.ecmwf.int/en/forecasts/dataset/ecmwf-reanalysis-v5
[6] https://cdip.ucsd.edu/m /products/? stn=154p1

of the International Hydrographic Organization and the Intergovernmental Oceanographic Commission[7]. GEBCO uses a combination of multibeam survey data and data interpolation to create a terrain model. The dataset is contained in a NetCDF format with a resolution of 15 arc seconds or 460 meters relative to the Mean Sea Level. Figure 3 shows the visualization of the processed bathymetry data from GEBCO's website[6] used in SWAN's non-stationary mode.

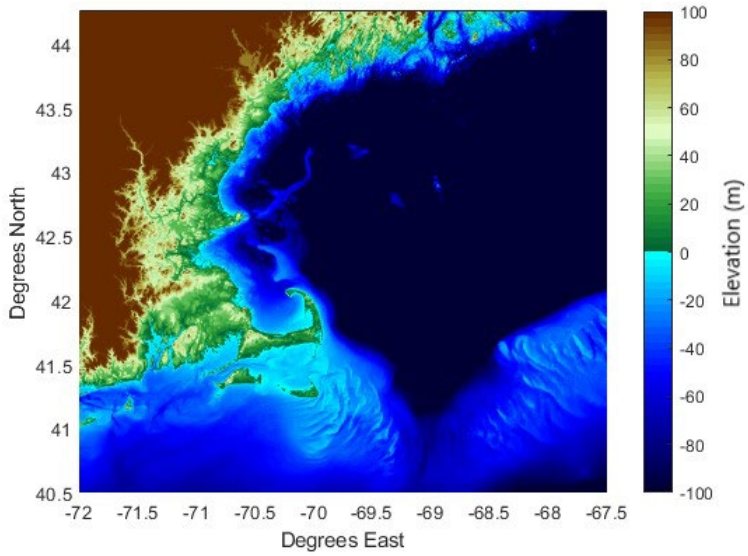

Figure 3. North Atlantic bathymetric plot from GEBCO

Bathymetric data used in the SWAN child grid comes from Coastal Relief Models from the National Centers for Environmental Information (NCEI)[7]. They integrate topographic and bathymetric data to generate elevation models covering onshore and offshore in the U.S. coastal zone. The integrated data were derived from hydrographic surveys, remote sensing, and interpolation. This data also includes regions around the U.S., such as Alaska, Hawaii, and Puerto Rico. The data was accessed through this link[8].

[7] https://www.gebco.net/data_and_products/gridded_ bathymetry_data/
[8] https://www.ncei.noaa.gov/products/coastal-relief-model

The datasets used for SWAN's stationary mode are from Coastal Relief Model Vol:1, which covers the Northeast Atlantic of the U.S. with a resolution of 3 arc-seconds or 90 meters, see Figure 4.

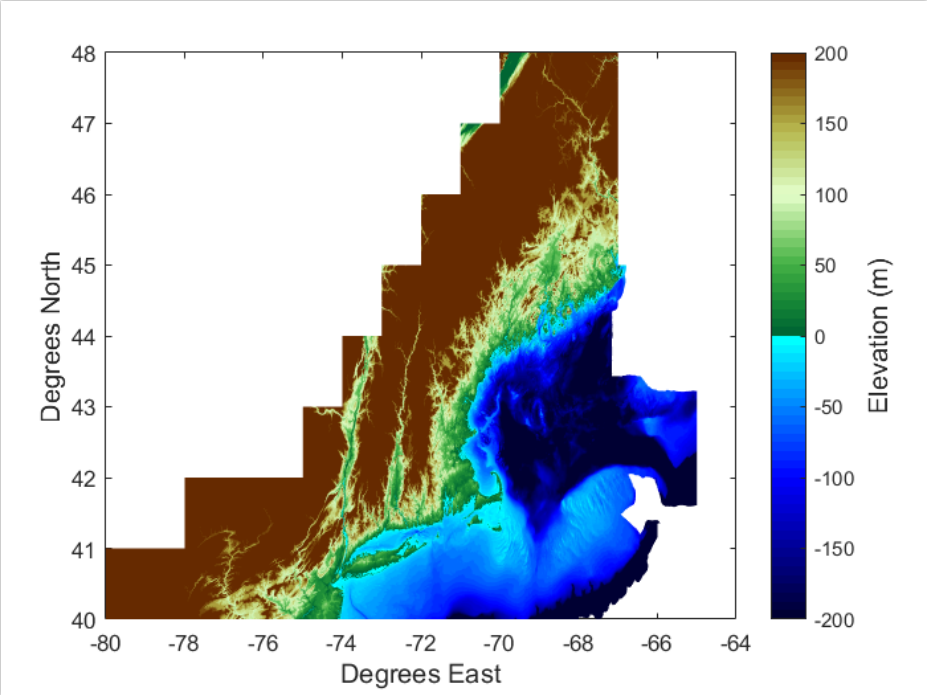

Figure 4. Northeast Atlantic bathymetric plot from Coastal Relief Model

WIS offers the public access to archived long-term wave information hindcast. Developed by the U.S. Army Corps of Engineers, WIS utilizes hindcast and spectral models to provide the public with information on waves and wind offshore of the U.S. coast. WIS consists of hourly wind and wave hindcast data from 1980 to 2020 in the area of study. WIS data from station 63101 will be used to force the wave boundary condition for the SWAN child domain. Figure 5. shows the interactive web portal for WIS stations in Rhode Island[9] that allows the user to download the datasets.

[9] https://wisportal.erdc.dren.mil/

Figure 5. WIS data station numbers and their respected locations near Rhode Island [7]

ECMWF operates as a research institute and an online web service, generating worldwide numerical weather predictions[10]. The ERA-Interim and ERA5 offer comprehensive time series data on various weather parameters, including waves, wind, temperature, and pressure. Each dataset is contained in a matrix with latitude, longitude, and time for each dimension respectively. Wind data from ERA-Interim was taken from October 1st to 31st, 2012, covering the Hurricane Sandy event with a 6 hours temporal resolution and spatial resolution of 0.75 degrees. The wind data consists of two sets of 10 meters elevation wind components U and V.

Another wind forcing used is the parametric wind models, which can better the core and also the wind field asymmetry of tropical cyclones or hurricanes (Olfateh et al., 2017). The parametric model captures two modes of wind speed asymmetry, azimuthal and radial. The radial asymmetry is captured using a double peak Holland Model (Cadone et al., 1994). The azimuthal asymmetry uses historical data from 21 different

[10] https://www.ecmwf.int/en/forecasts/dataset/ecmwf-reanalysis-v5

hurricanes to develop an empirical wind speed formula; details of this derivation can be found in (Olfateh et al., 2017). The data was acquired from a previous research (Hashemi et al., 2021). The data was previously utilized to investigate the impact of hurricanes on wind farm loads (Hashemi et al., 2021). This dataset will be employed in the SWAN parent domain to simulate Hurricane Sandy, and the results will be compared with the ECMWF dataset, specifically the SWAN-simulated waves based on ECMWF wind data. This comparison is to see which wind forcing best aligns with the observed data and consequently serves as model validation.

CDIP constitutes a comprehensive network that monitors waves and beaches along the United States coastlines. Over the years, the program has compiled an extensive and publicly accessible environmental database for the public[11]. Due to its proximity to the study area, CDIP 154 will be used to validate the SWAN non-stationary model. Figure 6 shows the significant wave height time series observed during Hurricane Sandy from the CDIP 154 Block Island, RI buoy used in this study.

[11] https://cdip.ucsd.edu/m /products/? stn=154p1

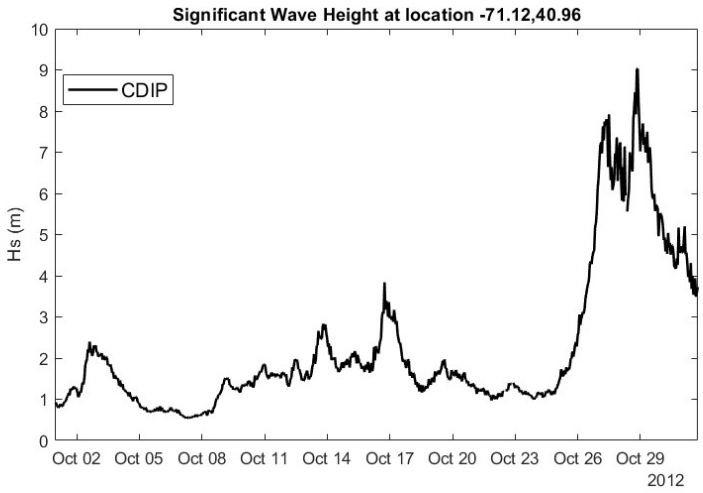

Figure 6. The significant wave height time series observed during Hurricane Sandy from the CDIP 154 Block Island, RI[10]

Data collected by the Woods Hole Group as part of the regional sediment management (RSM) will be used to validate the SWAN child domain (Woods Hole Group, 2012). Woods Hole Group is a company that focuses on solving environmental and coastal issues. They conducted a regional sediment management, a system-based methodology, focusing on comprehensively managing and resolving sediment-related problems (Woods Hole Group, 2012). As part of the RSM study in Rhode Island, three offshore wave buoys (East, Center, and West) were deployed from July 30, 2010, to September 29, 2011, for over 10,000 hours of wave data was collected (Woods Hole Group, 2012). The latitude and longitude coordinates of the west, center, and east buoy are (41.31, -71.79), (41.34, - 71.65), and (41.36, -71.54), respectively. Each buoy is located approximately 1.6 km off the coast of Matunuck, RI, with 10.46 km between buoys.

Figure 7 shows the approximate location of the three buoys used in SWAN child domain validation (Woods Hole Group, 2012).

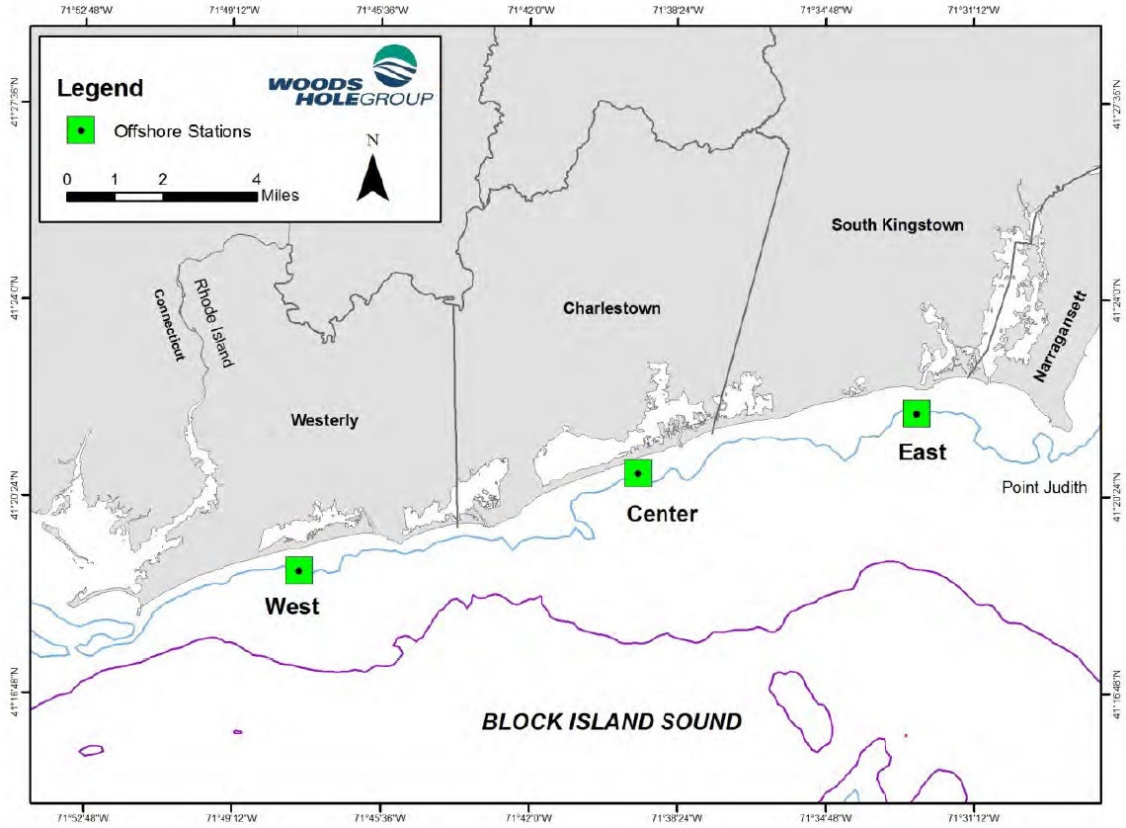

Figure 7. An approximate location of the buoys which were used to validate the SWAN child domain (Woods Hole Group, 2012).

2.2.2. SWAN Stationary and Non-stationary Model Setup

SWAN was used to model the waves along the southern Rhode Island coastline. Two modes of SWAN will be used in this study, non-stationary and stationary. SWAN stationary mode assumes the wave conditions to be constant over time, while non-stationary mode simulates wave conditions that evolve over time. The non-stationary mode provided more accurate simulations but is more computationally demanding. Two domains will be used in this study: the parent and child domains. The non-stationary mode will be used for the SWAN parent domain, and the stationary mode will be used for the SWAN child domain. The SWAN child domain will be nested inside the parent domain, which is done so that there is minimal spatial variability across the SWAN child domain boundary. Two SWAN domains (parent grid and child grid) and one XBeach domain are shown in Figure 8.

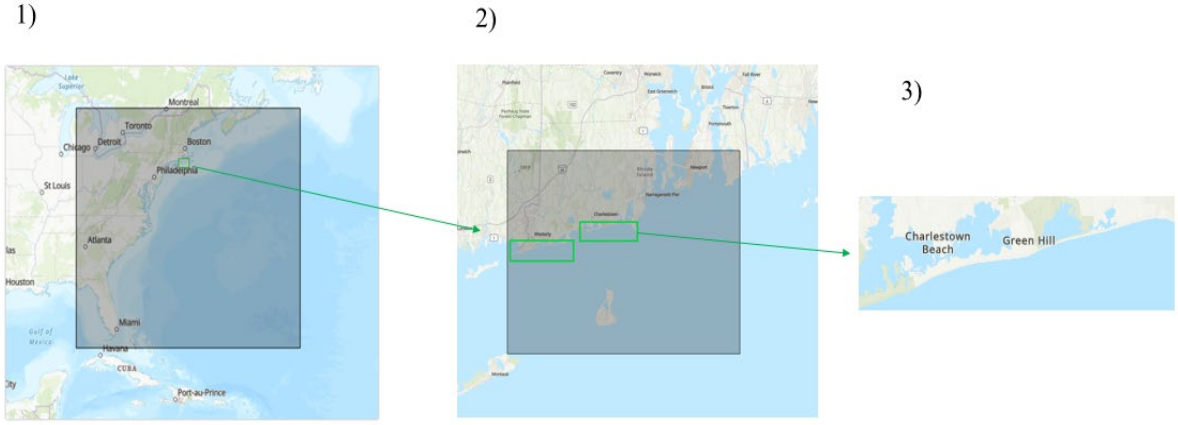

Figure 8. Modeling domains. 1) SWAN non-stationary (parent) domain in grey. 2) SWAN stationary (child) domain in grey. 3) XBeach domains in green.

The parent grid was set up in a SWAN non-stationary mode to assess the spatial variability of wave conditions along the boundaries. The non-stationary mode allows the user to simulate a time-dependent wave spectrum. The domain is set up in the North Atlantic in a spherical mode with a nested boundary condition as an input into the smaller child grid, as shown in Figure 8. The parent grid resolution is 0.125 degrees by 0.125 degrees. The time interval of each computation step is set to 6 hours.

ECMWF commonly uses data for forecasting that contains wind speeds over the region of storms (Dee et al., 2011). The model will be forced with EMCWF wind data. This is beneficial for the study since the model can use the information surrounding the storm to simulate wave conditions based on the wind parameters. The model input has two 10 meters elevation wind components, U and V. The U components refer to the west to east direction, while the V component is the north to south. ERA-Interim data was taken from October 1st to 31st, 2012, during the Hurricane Sandy event with 0.75 degrees resolution and 6 hours temporal resolution.

The bathymetry data for the SWAN parent grid was taken from GEBCO (Mayer et al., 2018). The datasets were provided with the spatial resolution of 15 arc-second intervals, roughly 460 meters[12]. The data is then mapped into the North Atlantic area with coordinates of -120.0 degrees W to -50.0 degrees W and 20.0 degrees N to 50.0 degrees N. Since the waves were generated by wind forcing and the domain is relatively large, there is no wave boundary condition in the parent grid.

[12] https://www.gebco.net/data_and_products/gridded_bathymetry_data/

The SWAN child domain covers the southern coast of Rhode Island, with coordinates ranging from -71.90 to -71.30 W and 41.10 to 41.40 N (refer to Figure 9) with a resolution of 0.005 degrees by 0.00375 degrees in horizontal and vertical direction respectively. In this study, two simulations were carried out: one for extreme conditions during Hurricane Irene and another for average sea states. Both extreme and average scenarios utilized the same bathymetric data from the Coastal Relief Model's Volume 1.

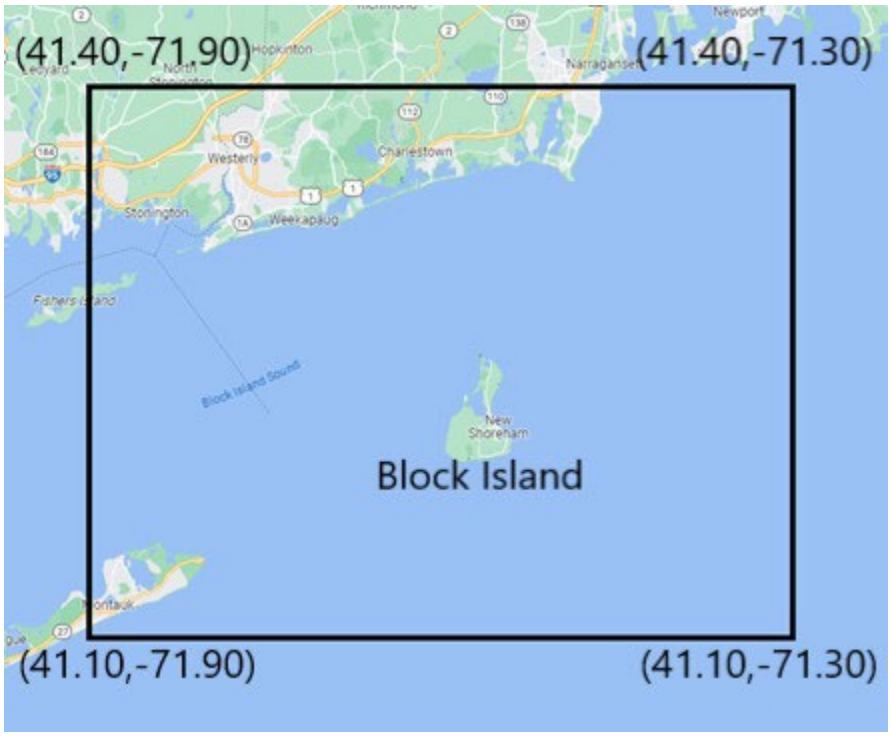

Figure 9. SWAN child domain

Spatial variability along the SWAN child domain will be analyzed using the SWAN parent model. If there is minor variability along the boundary from the SWAN parent model, it will further justify WIS data as a substitution since WIS data will force a constant boundary condition along the child domain. The variability along the boundary will be determined by plotting the time series of significant wave heights along the boundary of the SWAN child domain. Five different points along the boundary were

chosen: point W1 at (-71.90,41.20) on the west side of the boundary and point E1 at (-71.30,41.20) on the east side of the boundary. Points S1, S2, and S3 at (-71.80,41.10), (-71.50,41.10), and (-71.40,41.10), respectively, on the south boundary; see Figure 10 for the approximate location of each point.

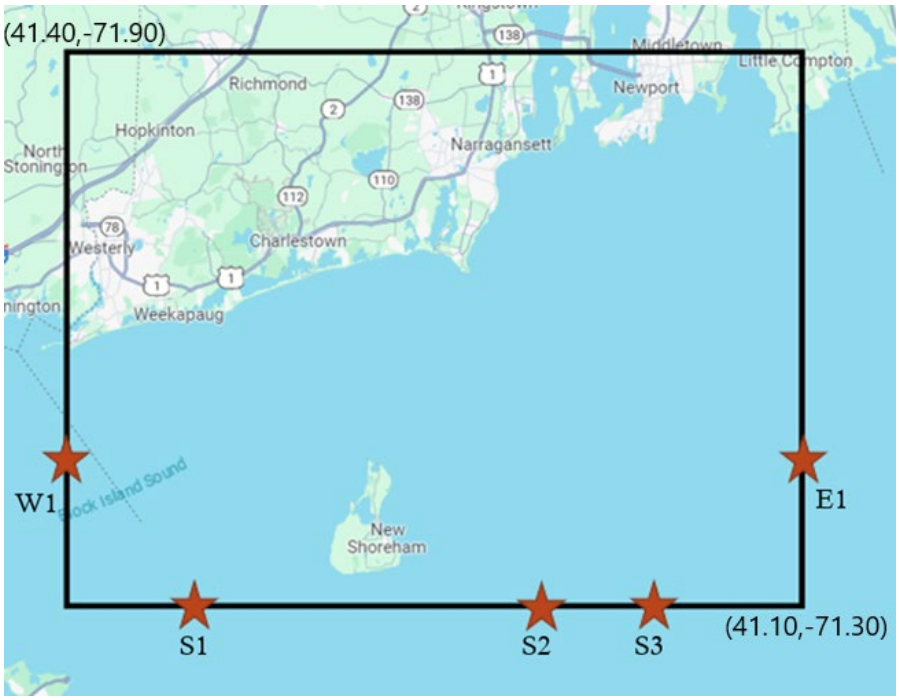

Figure 10. The location of five points along the boundary is where the wave height time series variability is compared: point W1 on the west side, point E1 on the east side, and points S1, S2, and S3 on the south side.

The boundary conditions will be forced from WIS data between August 1st and August 31st, 2011, during Hurricane Irene. Two different stationary SWAN simulations were run. The first stationary SWAN simulation used regular sea states as the boundary condition, and the second used extreme sea states. The first simulation's boundary condition was forced with mean significant wave height, mean wave period, mean wind direction, and mean wind speed from August 1st to August 14th of 2011. The second run was forced with peak significant wave height, peak period, maximum wind speed, and its associated direction from August 15th to August 31st during Hurricane Irene. The wind

and wave direction from the data was converted from nautical to cartesian convention to be consistent with SWAN. The time series plot of significant wave height *Hs* and peak period *T* from August 1st to August 31st during Hurricane Irene acquired from WIS data is shown in Figure 11.

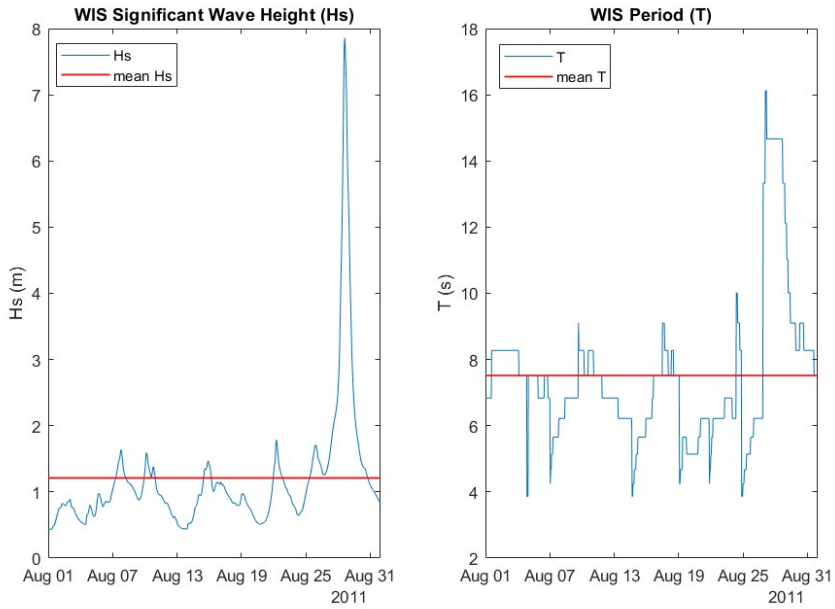

Figure 11. WIS time series in August 2011. The left and right plot show the time series in blue line of the significant wave height and the wave period respectively. While the red line shows the mean value of the significant wave height and period.

2.3. Validation and Results

Significant wave heights generated by the primary SWAN model were compared with those generated by ECMWF and observation data from CDIP buoy 154 or station 44097. The location of CDIP buoy 154 is illustrated in Figure 12. The results of the high-resolution SWAN run and the low-resolution SWAN run are shown in solid red and blue lines on Figure 13. SWAN results show a peak significant wave height of 4 m, while the observed significant wave height by CDIP is greater than 9 m.

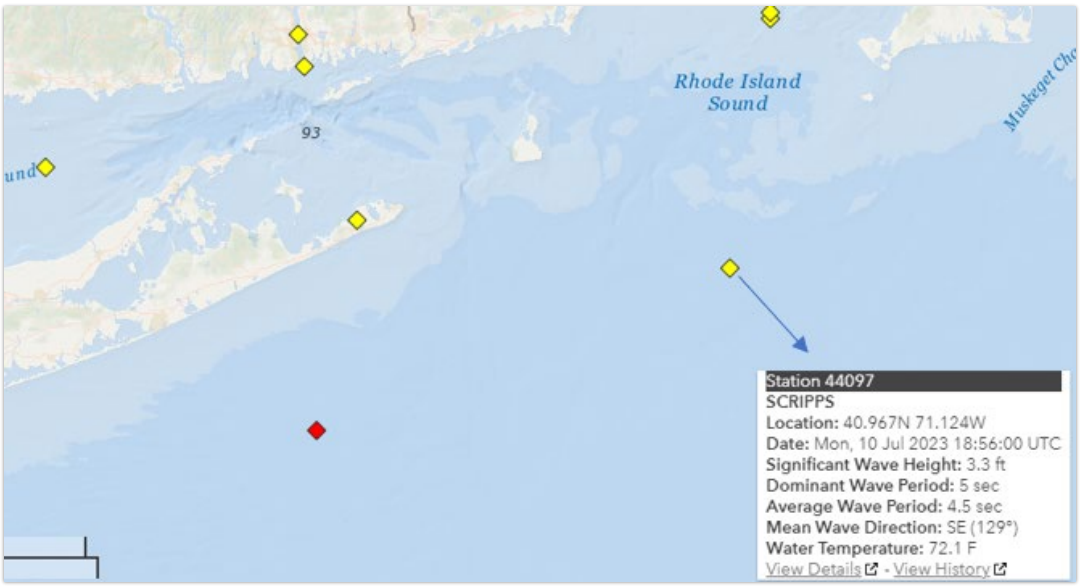

Figure 12. Location of the CDIP 44097 buoy used in SWAN.

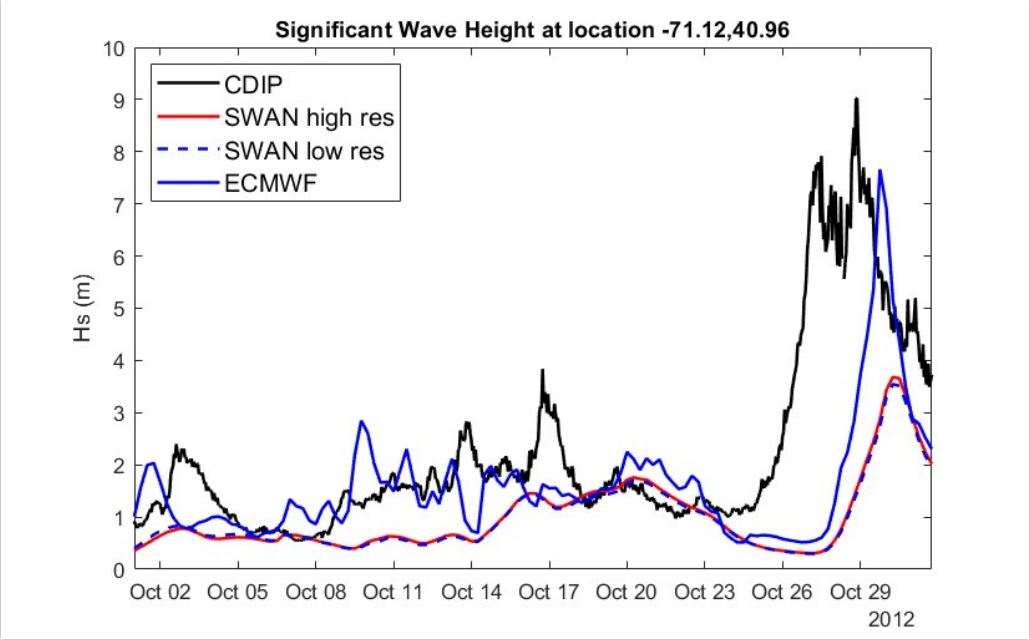

Figure 13. Comparison of significant wave height observed during Hurricane Sandy from CDIP 154 (solid black line) with low- resolution SWAN (dashed blue line) and high-resolution (solid red line) SWAN simulated significant wave height, and ECMWF simulated significant wave height data (solid blue line).

The maximum wind speed from ECMWF was recorded as 35.1 m/s, while the documented maximum wind speed during Hurricane Sandy was 51 m/s (Blake et al., 2013). The ECMWF data exhibited an underestimation of wind speed, as it lacks the inclusion of a synthetic vortex in the forecast model of hurricanes (Walsh et al., 1997).

Therefore, the discrepancy in simulated wave height versus the observed wave height may be attributed to the potential inaccuracies in the ECMWF wind data forcing used as input to the SWAN model. A different wind field from Hurricane Sandy was implemented using a parametric numerical hurricane model from (Hashemi et al., 2021). The parametric wind model included the asymmetry observed in the center of tropical hurricanes, as described in (Olfateh et al., 2017). This is done to evaluate whether this discrepancy is due to the ECMWF wind data forcing or a fault in the model setup.

Simulated waves from the parametric wind forcing are compared to the ECMWF, and CDIP observed data in Figure 14. The solid black, blue, and red dashed lines in Figure 14 represent the significant wave height from CDIP, ECMWF, and Parametric SWAN run, respectively.

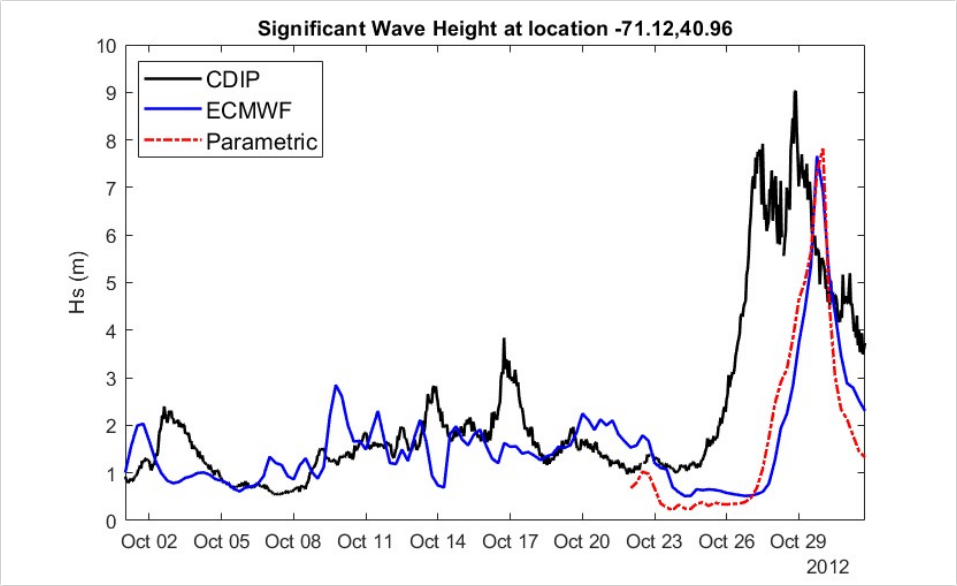

Figure 14. Comparison of significant wave height observed during Hurricane Sandy from CDIP 154 (solid black line) with SWAN's parametric wind simulated significant wave height (dashed red line) and ECMWF's simulated significant wave height (solid blue line).

SWAN parametric wind forcing in the dashed red and black lines is in good agreement with ECMWF (solid blue line) and the observed data from CDIP (solid black line). The peak significant wave height generated by SWAN parametric wind forcing is approximately 7.82 m, where ECMWF is 7.66 m. The error (in Figure 13) is due to ECMWF wind forcing. The significant wave height simulated by parametric wind forcing was also compared with WIS station ST63101. The comparison is shown in Figure 15 with CDIP in a solid black line, parametric SWAN run in a red dashed line, and WIS in a solid blue line.

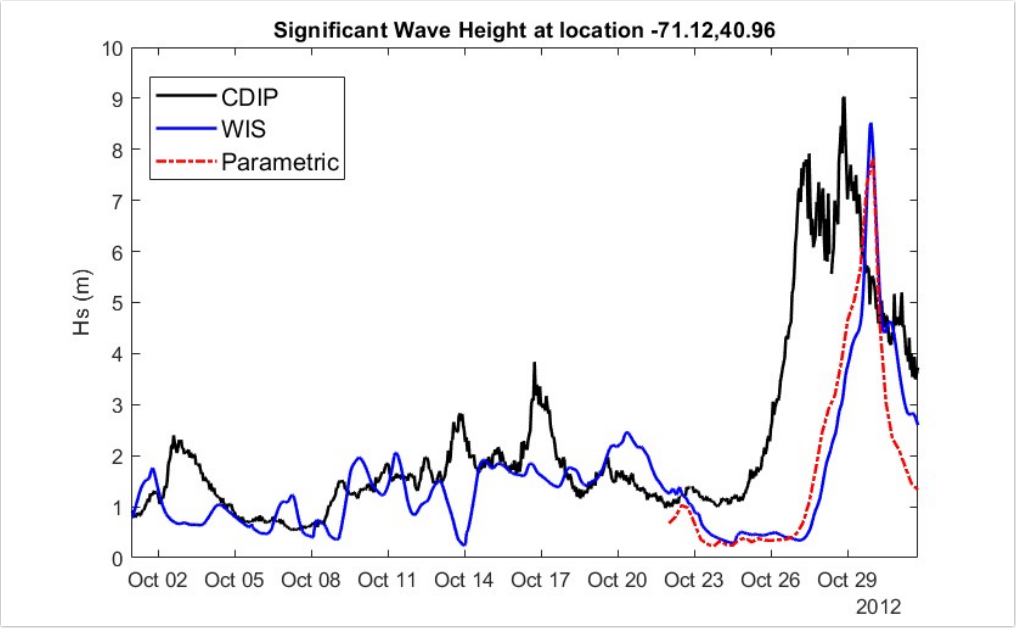

Figure 15. Comparison of significant wave height observed during Hurricane Sandy from CDIP 154 (solid black line) with SWAN's parametric wind simulated significant wave height (red dashed line) and WIS's hindcast data (solid blue line).

This result shows that the peak significant wave height simulated by WIS is approximately 8.57 m, while the SWAN parametric wind forcing simulated peak significant wave height is approximately 7.66 m. The SWAN parametric wind generated significant wave height is within 15 % agreement with the CDIP 154 location. Additionally, the WIS simulated wave height is in better agreement with the CDIP 154 buoy, with a percent error of 5.87%.

The time series of the significant wave height along the SWAN child boundary is plotted in Figure 16 (Refer to Figure 10 for location points along the boundary). The west boundary (W1) and east boundary (E1) are shown on the left of Figure 16 while the south boundary (S1, S2, S3) is shown on the right of Figure 16.

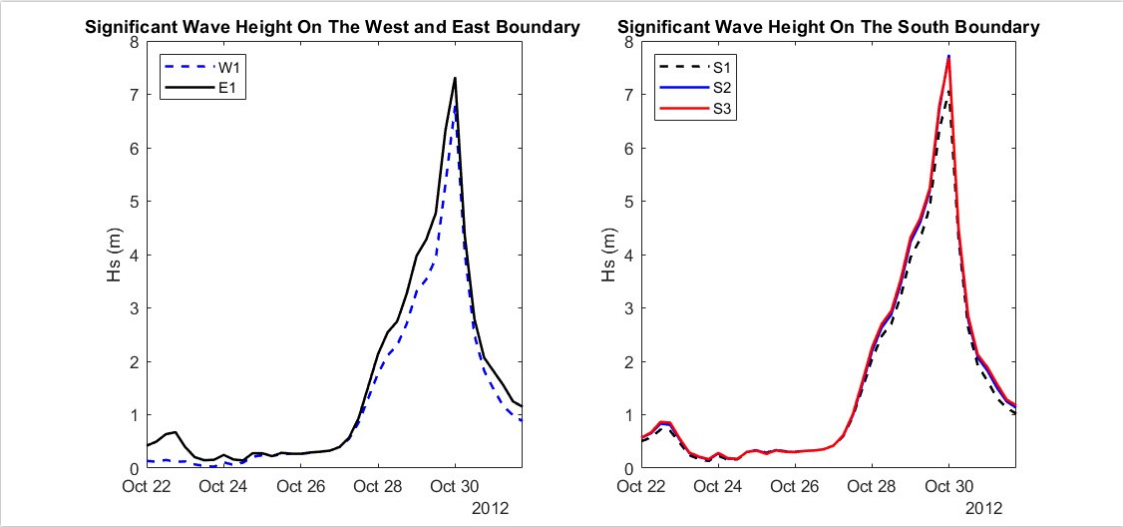

Figure 16. The time series of the significant wave height generated by SWAN's parametric wind at W1 and E1 are shown in blue dashed and solid black line on the (Left). The significant wave height for the south boundary at S1, S2, and S3 is shown in the dashed black, solid blue, and solid red lines, respectively (Right). For locations of S1, S2, S3, W1, and E1 refer to Figure 10.

The significant wave height time series along the boundary shows minor variability with a mean of 7.32 m and a relative standard deviation of 6%. Therefore, wave data from the WIS station will be used to force the boundary condition on the SWAN child domain as a more efficient method.

The simulated wave height and period from the SWAN child grid were compared to those from the Woods Holes Group report on RSM study in Rhode Island (Woods Hole Group, 2012). The data used for validation is taken from the west and center buoy from August 1, 2011, to August 31, 2011. The east buoy was excluded from the analysis since it contains no data after July 23, 2011. The data shows that the dominant wave direction is 160 to 200 degrees in Nautical convention, significant wave height is shown to be between 0.22 m to 1.5 m with a peak of 4 m during Hurricane Irene, and the peak period is between 5 to 10 seconds (Woods Hole Group, 2012). The mean significant

wave height (Hs) observed by the center and the west buoy is 0.68 meters and 0.67 meters, respectively. While SWAN simulated a significant wave height of 0.76 meters at the location of the center buoy and 0.81 meters at the location of the west buoy. In comparison, SWAN overestimated the significant wave height at the center and west buoy by 11.34% and 20.93%, respectively. The mean period (*T*) observed by the center is 4.5 s and 4.4 s for the west buoy. While SWAN simulated the wave period of 3.9 s at the location of the center buoy and 4.3 s at the location of the west buoy. This shows an error of 14.15% on the center buoy and 1% on the west buoy. A summary of the result is shown in Table 1.

Table 1. Summary of SWAN mean scenario simulations compared to observed buoy data from August 1st to 14th. Refer to Figure 7 for buoy locations.

	Observed Mean Hs	SWAN Mean Hs	Percent Error	Observed Mean T	SWAN Mean T	Percent Error
Center Buoy	0.68 m	0.76 m	11.34%	4.5 s	3.9 s	14.15%
West Buoy	0.67 m	0.81 m	20.93%	4.4 s	4.3 s	1%

SWAN wave simulation results for the extreme scenario were compared to those of the center buoy. A time series plot of the observed data from the center buoy and SWAN peak significant wave height and period is shown in Figure 17. The result from the center buoy shows a 5.77% error with an observed data of 4.08 m, while the SWAN simulated significant wave height is 4.33 m.

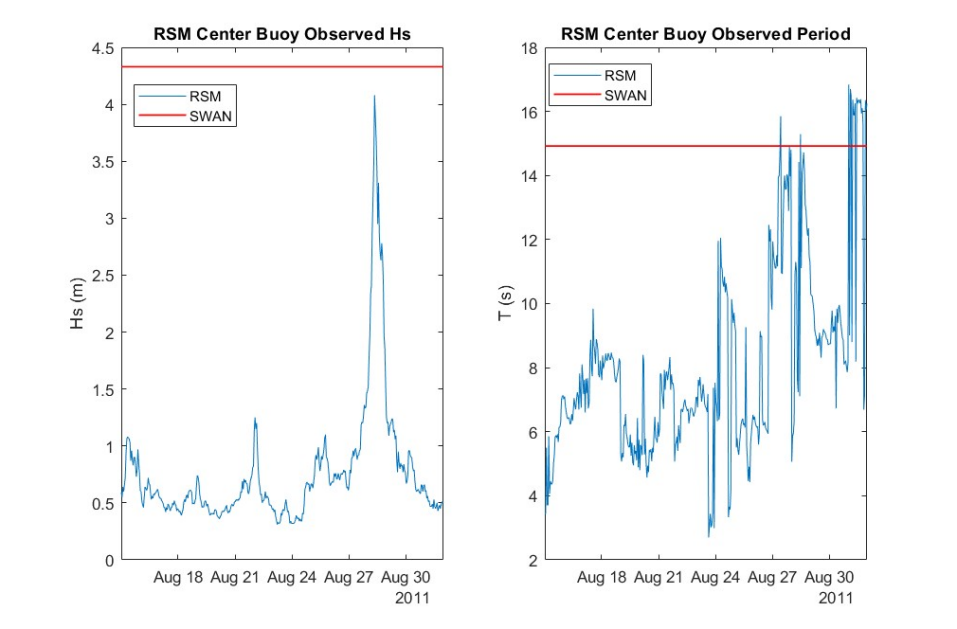

Figure 17. The significant wave height simulated by SWAN is 4.33 m, as shown on the red line, compared to the Woods Hold Group (RSM) observation data of 4.08 m from the center buoy (left) (See Figure 7 for RSM buoy location). The peak period of 14.92 s is compared to the observed period on the red line (right).

SWAN wave simulation results for the extreme scenario were also compared to the West buoy. Figure 18 shows a time series plot of the observed data from the West

buoy and SWAN peak significant wave height and period. The result from the West buoy has an error of 1.58% with an observed data of 3.75 m compared to SWAN's 3.81 m.

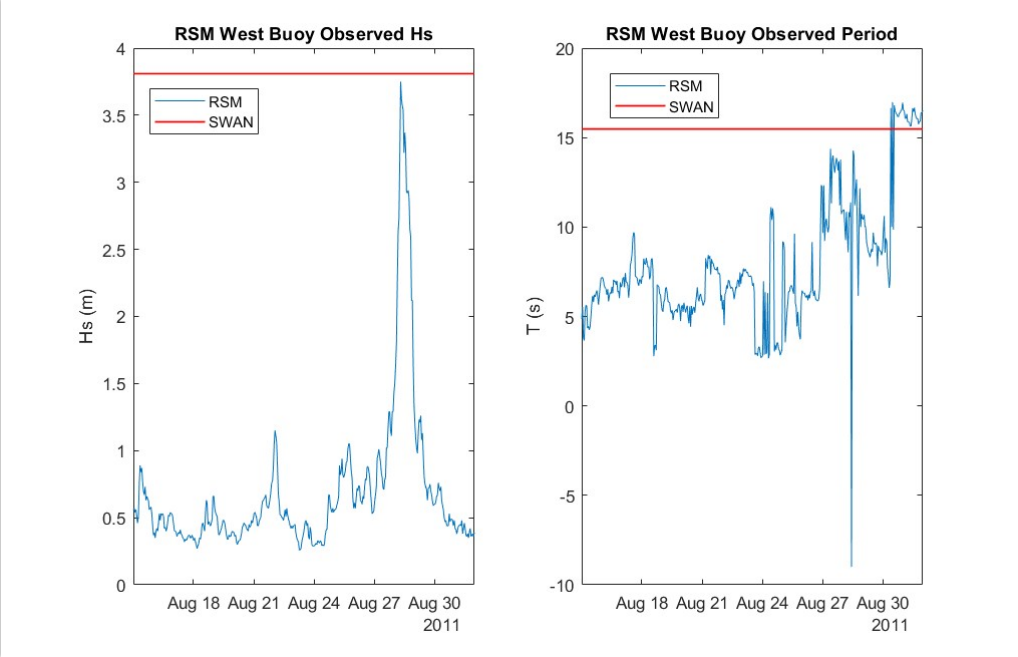

Figure 18. The significant wave height simulated by SWAN is 3.81 m, as shown on the red line, compared to the Woods Hole Group (RSM) observation data of 3.75 m from the west buoy (See Figure 7 for RSM buoy location). The peak period of 15.48 s is compared to the observed period on the red line (right).

2.4. Wave Model Discussion

Parent SWAN's parametric wind simulation of significant wave heights showed minor variation between five points along the southern, western, and eastern boundaries of the child domain (See Figure 10 for point locations). The distance between the three points along the south boundary is approximately 0.30 degrees, while the east and west sides are approximately 0.60 degrees apart. The significant wave height on the east boundary (E1) is 6.78 m while the west boundary (W1) is 7.32 m (see left side of Figure 16). This value differs by 7.9%. The significant wave heights along the three points on the south boundary S1, S2, and S3 (refer to the right side of Figure 16) is 7.07 m,7.74 m, and 7.68 m respectively. These significant wave heights varied by less than 10% along the south boundary. The small variation observed across the boundary implies a correspondingly low level of spatial variability.

The standard deviation of significant wave heights for the five points along the boundary is 0.41 m, with a mean of 7.32 m and a relative standard deviation of less than 6%. Additionally, as depicted in Figure 15, SWAN's non-stationary parametric simulation is consistent with WIS wave simulations, further validating the use of WIS as a boundary condition for the SWAN child domain.

2.5. Wave Model Conclusion

Non-stationary SWAN simulations show that parametric with forcing is more accurate than EMCWF wind forcing when compared to the observed data from CDIP (See Figure 14). This is because ECMWF cannot accurately simulate the hurricane's core near its eye.

The SWAN parametric wind simulation results show minimal wave variation along the boundary, with a standard deviation of 0.41 m, a mean of 7.32 m, and a relative standard deviation of less than 6% across five points. This confirms that WIS is an effective substitute for the SWAN parent grid, serving as a SWAN child boundary condition to save computational time. The SWAN child simulation with WIS boundary conditions resulted in an error of 1.58% for the west buoy and 5.77% for the center buoy. These results validate the model for further use in XBeach, as the errors are consistently below 6%.

3. Chapter III. Sediment Transport Model

3.1. XBeach Introduction

XBeach is an open-source 2-D (two-dimensional) physics-based model that simulates hydrodynamic and morphodynamic processes (Roelvink et al., 2015). Some examples of hydrodynamic processes simulated by XBeach include short wave generation, long wave generation, and wave transformation. Some examples of morphodynamic processes simulated by XBeach include sediment transport, bed slope update, the effect of vegetation, and dune avalanching. XBeach contains a hydrostatic mode and a non-hydrostatic mode. The hydrostatic mode solves a group of short waves separately from long waves and morphological changes. Short wave transformation includes wave refraction, shoaling, and wave breaking, while long wave or infragravity wave transformation includes wave generation, propagation, and dissipation. The non-hydrostatic mode uses non-linear wave equations and depth-average non-hydrostatic pressure corrections to solve the waves, which allows the model to propagate and decay each wave. The hydrostatic mode was used in this numerical experiment since the focus was on the swash zone. The model uses a coordinate system where the x-axis is oriented approximately perpendicular to the shore and the y-axis is oriented approximately parallel along the coast. The input grid must be in a curvilinear system. However, a rectangular grid is possible using coordinate transformations with an origin point and an angle with respect to the curvilinear grid. The axis orientation of the XBeach model can be seen in Figure 19. This oriented grid is called the local grid. The local grid coordinate system is relative to the world grid coordinate system. The coordinates in the world grid are defined as (X,Y), the local coordinates is defined as (x_L,y_L), and the origin point for

the local grid is defined as (x_{ori},y_{ori}), and the angle counterclockwise from the positive X-axis is α (Roelvink et al., 2015).

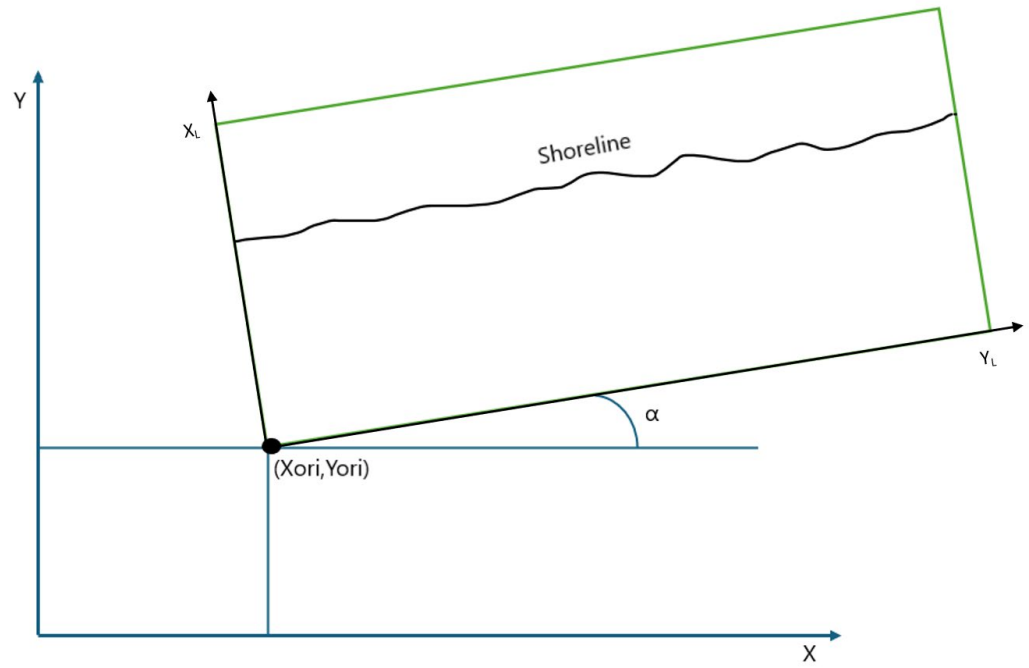

Figure 19. XBeach grid orientation based on Roelvink et al., 2015.

XBeach uses the advection-diffusion equation assuming *C* is the depth-averaged sediment concentration and D_h is the sediment diffusion coefficient to model sediment transport. The sediment transport rate is calculated using q_x, and q_y in the x and y directions respectively, as shown in Equation 9 and 10 respectively. Variables *h* and *t* represent the water depth and time, respectively.

$$q_x(x,y,t) = \frac{\partial hCu^E}{\partial t} + \frac{\partial}{\partial x}\left(D_h h \frac{\partial C}{\partial x}\right) \tag{9}$$

$$q_y(x,y,t) = \frac{\partial hCv^E}{\partial t} + \frac{\partial}{\partial y}(D_h h \frac{\partial C}{\partial y}) = 0 \tag{10}$$

It is beyond the scope of our discussion to offer a comprehensive review of XBeach, however, a detailed derivation can be found in Roelvink et al., 2015. Two important

factors in calibrating the XBeach model are the morphological factor f_{mor} and *facua*, Υ_{ua}. *Facua* considers the wave skewness and asymmetry of the wave's orbital velocities.

$$\frac{\partial z_b}{\partial t} + \frac{f_{mor}}{(1-p)}\left(\frac{\partial q_x}{\partial x} + \frac{\partial q_y}{\partial y}\right) = 0 \tag{11}$$

where z_b is bed level, p is the porosity, f_{mor} is a factor added to accelerate the computational time of the morphological changes.

3.2. Methods

XBeach domain for this study is located at RI5: Green Hill Beach, shown in Figure 2. The computation grid input is defined as nx and ny. As mentioned in the previous section, the x-axis is perpendicular to the shoreline, while the y-axis is parallel to the shoreline. The bathymetry used for XBeach is from NCEI and is used in Global DEM Global Mosaic with a resolution of 1/9 arc second, around 3 meters. The size of the computation grid is nx = 199 and ny = 299, with a resolution of 10 m and 8.7 m, respectively.

The spatial Manning coefficient was used for the friction input. The data was taken from Schambach et al., 2018, which was derived from Rhode Island 2011 land use and land cover data. The study employed the XBeach numerical model to simulate a storm with a 100-year return period along the southern shore of Rhode Island, near Charlestown Beach which falls inside the XBeach domain in this study.

XBeach was nested inside the SWAN child domain. The SWAN boundary condition was forced with WIS data during Hurricane Sandy. The peak period, peak significant

height, maximum wind, and wind direction were used as input to SWAN. The boundary condition generated from SWAN was rotated by 90 degrees to be consistent with the XBeach grid.

Median sediment grain size, storm surge, and tide were also included in this study. Tide and storm data were taken from NOAA Newport RI tidal station 8452660. This location was chosen for its proximity to the study area. The median sediment grain size used is acquired from the study in mitigation of coastal erosion along the southern shore of Rhode Island as part of the 2022 senior capstone (Amante et al., 2020). The median sediment grain size is 0.41 mm.

3.3. XBeach Validation and Results

3.3.1. XBeach Validation

LiDAR topographic data from 2011 and 2012 were used to validate the XBeach simulation after Hurricane Sandy. LiDAR, which stands for Light Detection and Ranging, is a remote sensing technology that uses laser light to measure distances and generate precise, three-dimensional information about the shape and characteristics of objects and surfaces. The source of the LiDAR data is from NOAA[13]. They offer a customized download feature that allows users to access up to 1.5 billion LiDAR data points. The elevation changes from the LiDAR data from 2011 to 2012 are plotted in Figure 20 below. These datasets were chosen to assess morphological changes before and

[13] https://www.coast.noaa.gov/dataviewer/#/

after the impact of Hurricane Sandy.

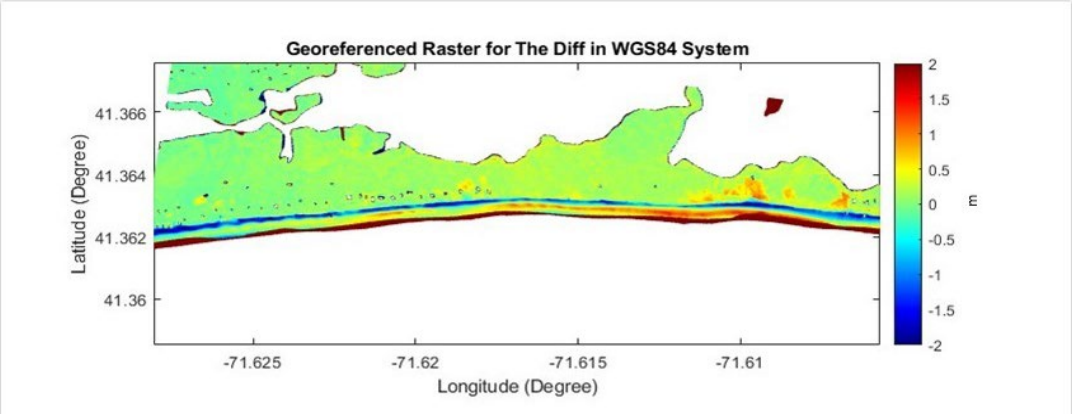

Figure 20. LiDAR elevation changes from 2011 to 2012. The color gradient indicates elevation changes in meters, with positive values indicating sediment deposition and negative values indicating sediment erosion.

XBeach was used to simulate the morphological processes before and after Hurricane Sandy, as shown in Figure 21. The first two plots show the bathymetry before and after Hurricane Sandy, respectively. The resulting elevation change between these two snapshots in time is shown in the third plot.

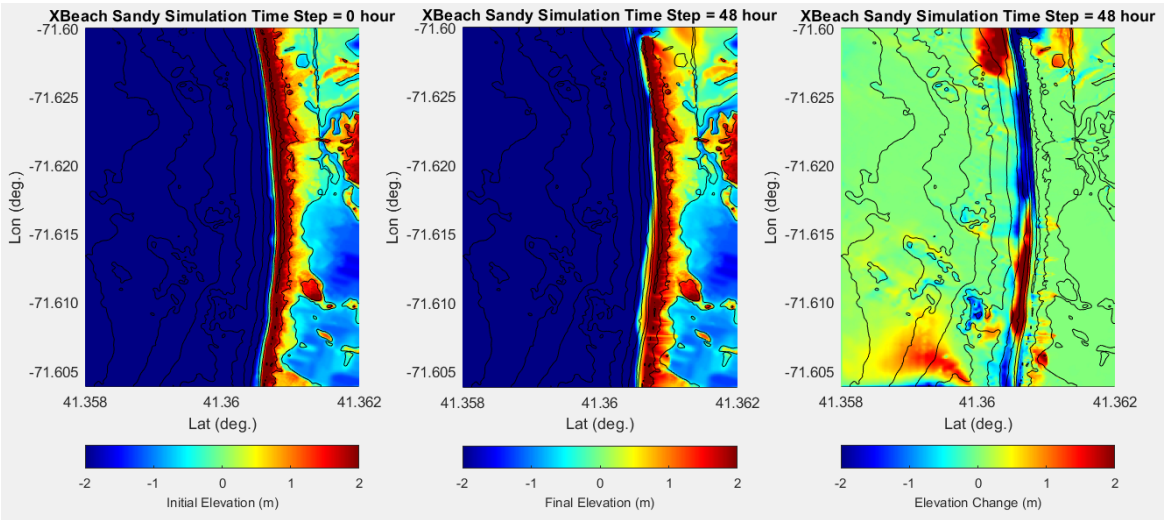

Figure 21. Plot of XBeach simulation elevation before Hurricane Sandy (left), elevation after Hurricane Sandy (middle), and elevation changes (right). The color gradient indicates elevation in meters, with positive elevation in blue and negative elevation in red.

The elevation changes from XBeach Hurricane Sandy simulation are then compared to LiDAR elevation changes from 2011 to 2012 is then. Figure 22 also shows the qualitative trend of sediment transport simulated by XBeach (bottom of Figure 22), compared with LiDAR elevation changes from 2011 to 2012 (top Figure 22). Notably, XBeach shows a trend in elevation changes that aligns with the LiDAR data. Specifically, along the coastline spanning -71.62 degrees to -71.61 degrees, there is sediment being transported offshore in both cases. Additionally, a comparable overwash regime is observed between -71.615 degrees to -71.61 degrees. The white area visible on the top of Figure 22 indicates regions where LiDAR data were not available.

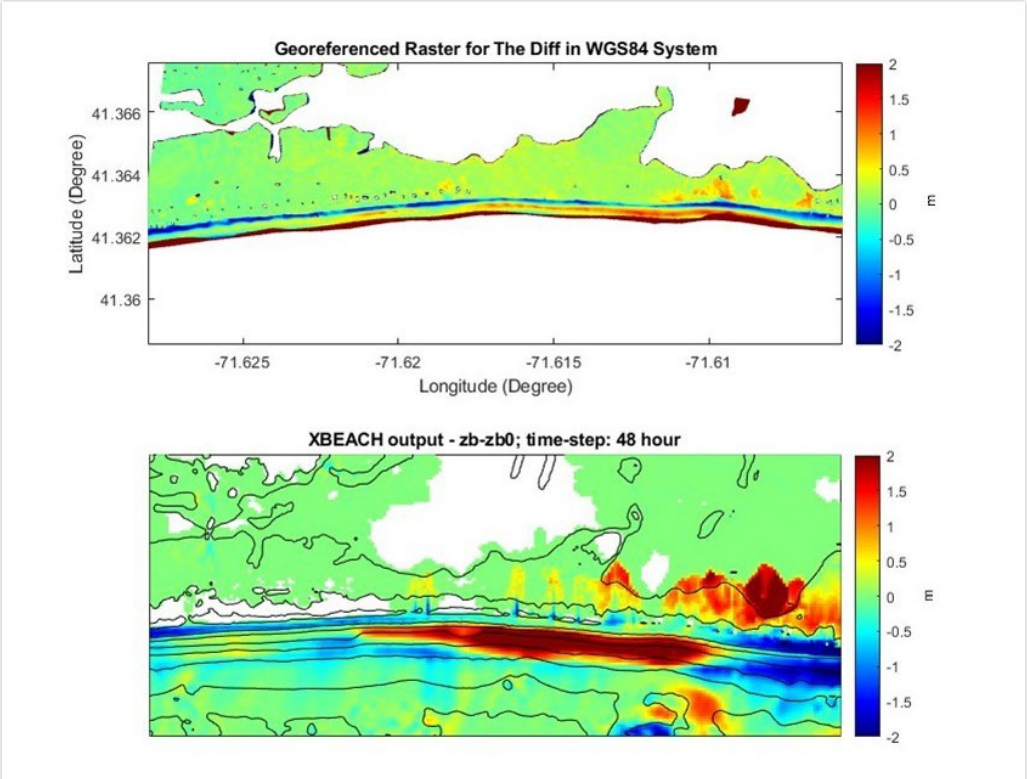

Figure 22. LiDAR elevation change in meters (top) compared with XBeach elevation change in meters (bottom) before and after Hurricane Sandy. The color gradient indicates elevation changes in meters, with positive values indicating sediment deposition and negative values indicating sediment erosion.

Despite the several similarities, there are also a few differences between the simulation and the LiDAR data. There are several reasons for these discrepancies. Firstly, the LiDAR data used for validation covers 2011 and 2012, as data directly before and after the storm are unavailable. This gap may allow the natural post-storm recovery to occur during this period. Furthermore, our simulation lacks consideration of sediment grain size variability due to the lack of data. Additionally, the XBeach model does not account for changes in vegetation as the beach evolves with storm events (Schambach et al., 2018).

3.3.2. Simulation of Other Storms by XBeach

XBeach simulations were used to represent storms for each season: nor'easter in the Spring of 2013, nor'easter in the Fall of 2012, Hurricane Sandy in the Fall of 2012, and Hurricane Irene in the Summer of 2011. Hurricane Sandy and Hurricane Irene were selected to align with available validation data. Additionally, the nor'easters of 2012 and 2013 were chosen to represent seasonal storms in the spring and fall that impacted New England. The wave conditions of each storm are shown on Table 2. The XBeach simulation for Hurricane Irene is shown on the left section of Figure 23 and the simulation of Hurricane Sandy is shown on the right of Figure 23.

Table 2. Various wave conditions for each storm simulated by XBeach.

Storm	Peak Hs (m)	Peak Tp (s)	Peak Wave Direction in Cartesian (degrees)
Hurricane Sandy	8.5	14.7	138.5
Hurricane Irene	7.9	16.1	102.9
Nor'easter 2012	4.5	10.0	195.6
Nor'easter 2013	4.4	13.3	185.5

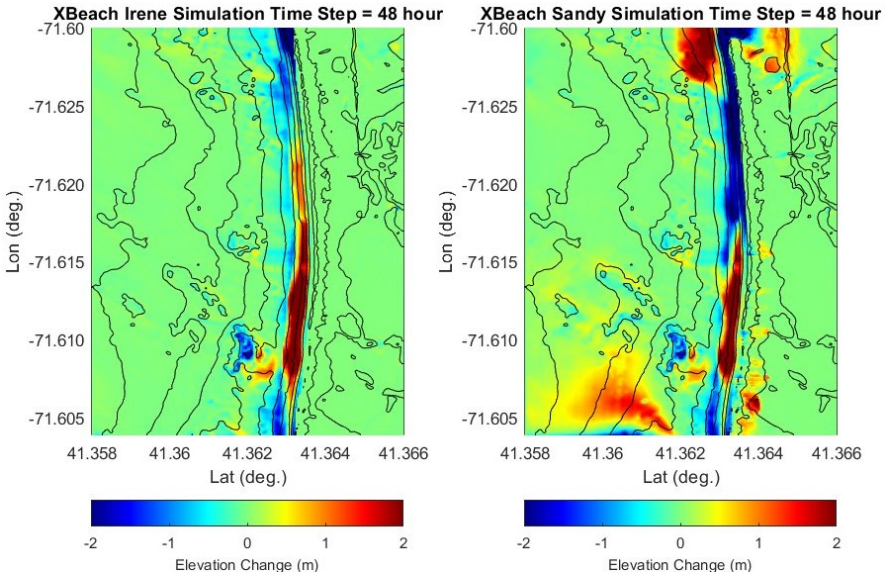

Figure 23. XBeach simulation for Irene (left) and Sandy (right). The simulations show sediment deposition in red and erosion in blue.

The simulations depicted in Figure 23 illustrate sediment deposition along the range of -71.615 degrees to -71.605 degrees in both cases. Nonetheless, Hurricane Sandy exhibits greater offshore sediment transport between 41.358 degrees and 41.362 degrees on both the east and west sides. Sediment appears to be trapped on the headlands at 41.358 degrees to 41.362 degrees on the west side. Another significant contrast is observed in the Hurricane Sandy simulations, which show sediment deposition inland with an overwash regime. This is attributed to surges and wave height differences between Hurricane Sandy and Hurricane Irene. Additionally, differences can be seen

from -71.62 degrees to -71.60 degrees, Hurricane Sandy simulation shows sediment erosion, whereas Hurricane Irene shows sediment deposition.

Another set of simulations were run during the nor'easter during the spring and fall seasons, as seen in Figure 24, on the left-hand side, displays the nor'easter 2013 simulation, while the right-hand side displays the nor'easter 2012 simulation.

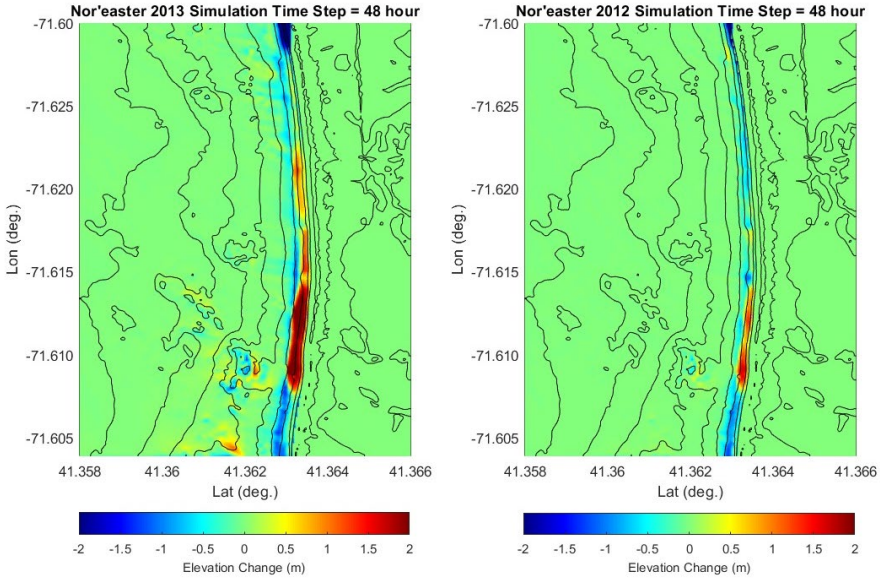

Figure 24. XBeach simulation for nor'easter 2013 (left) and nor'easter 2012 (right). The simulations show sediment deposition in red and erosion in blue.

Both scenarios show sediment deposition along the range of -71.615 degrees to -71.605 degrees. A slight cross-shore transport is noticeable between 41.360 degrees and 41.362 degrees on the east side, with more sediment deposition observed between -71.620 degrees and -71.65 degrees. While the deposition trend remains consistent, the significant difference lies in the magnitude of sediment transported. Another difference is in sediment erosion. The nor'easter 2012 simulation shows sediment erosion from -71.615 degrees to -71.620 degrees, whereas the nor'easter 2013 simulation shows sediment deposition.

In Figure 25 XBeach's simulations are presented, featuring the left plot depicting nor'easter 2013, the middle plot showcasing Hurricane Irene, and the right plot illustrating Hurricane Sandy. The purpose is to compare sediment deposition across multiple seasons: spring, summer, and fall, respectively. Sediment deposition remains consistent in the range of -71.615 degrees to -71.605 degrees across all three simulations. Hurricane Sandy simulation shows additional sediment deposition on top of the domain from -71.60 degrees to -71.625 degrees in front of the coastline and behind the coastal pond.

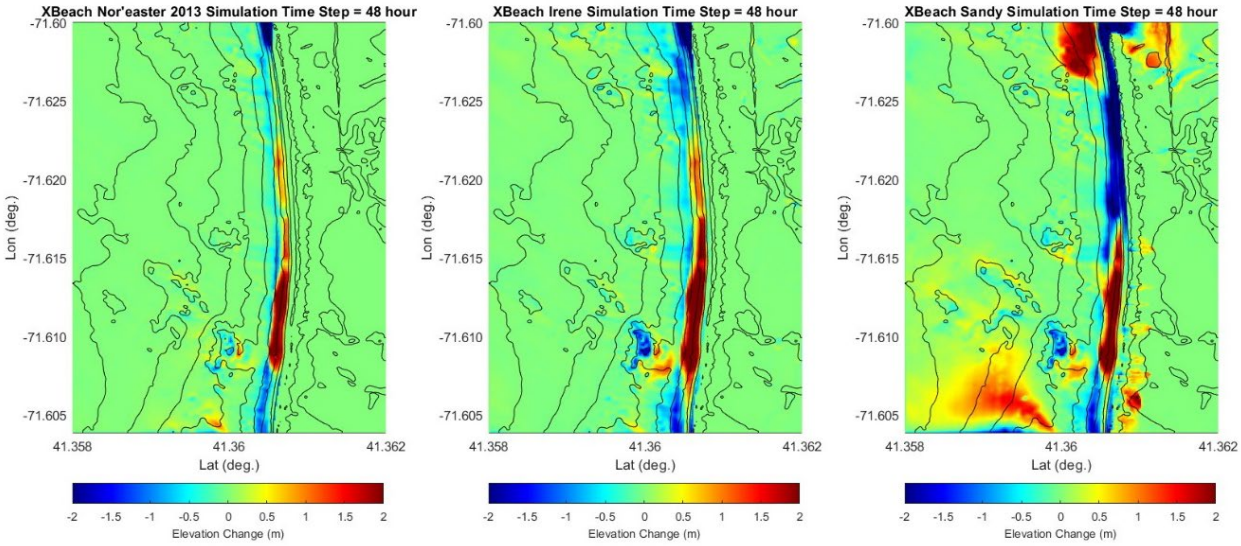

Figure 25. XBeach simulation for nor'easter 2013 (left), Irene (middle) and Sandy (right). The simulations show sediment deposition in red and erosion in blue.

Sediment erosion can be seen from the geographical west of the beach from -71.60 degrees to -71.62 degrees. Hurricane Irene and the nor'easter of 2013 simulations show similar erosion trends with differences in intensities, while Hurricane Sandy shows additional erosion behind the coastal pond on top of the domain.

While simulations of Hurricane Sandy and the nor'easter 2013 show similar trends in sediment transport, the key difference lies in the magnitude. Hurricane Sandy stands

out with significantly more cross-shore transport and sediment deposition inland. The total elevation change in sediment deposition and erosion for the Hurricane Sandy simulation is 292.21 m and 3454.02 m, respectively, within a domain of 5.20×10^5 m^2. Compared to the nor'easter 2013 simulation, the total elevation change in sediment deposition and erosion is 12.54 m and 177.91 m, respectively.

As depicted in Figure 25, nor'easter 2013 occurred in the spring, while Hurricane Irene occurred in the summer of 2012. Despite the seasonal variations, both events show similar sediment deposition patterns from -71.615 degrees to -71.605 degrees on the east side of the beach. This suggested that the sediment transport in this area is dominated by waves.

3.4. XBeach Simulations Discussion

Sediment transport in the nearshore is a function of beach profile, dune profile, sediment grain sizes, bathymetry, wave climates, storm surges, and tides. This study primarily focuses on analyzing wave climates, storm surges, tides, and bathymetry as part of the model input. Sediment is expected to be trapped inside the headlands within each barrier system, with the amount of transported sediment being influenced by the storm intensity in each season.

The XBeach simulation incorporated wave conditions, storm surges, and tides from various storms, including Hurricane Irene (Summer 2011), Hurricane Sandy (Fall 2012), and nor'easter storms in Fall 2012 and Spring 2013. Hurricane Sandy simulation shows that most sediment was transported offshore and inland. Sediment is shown to be trapped between the two headlands on the west and east sides of the domain. While

sediment deposition from a collision regime at -71.615 degrees to -71.605 degrees remained consistent for all simulated storms. Variations were observed along the west coastline between -71.615 degrees and -71.620 degrees. Notably, the nor'easter storm in the spring of 2013 and Hurricane Irene in the summer of 2011 show an increased sediment deposition, whereas Hurricane Sandy and nor'easter of 2012 show sediment erosion in that specific area. Additionally, across all four simulations, Hurricane Sandy is the only event dominated by an overwash regime, with sediment observed to be deposited in the Green Hill pond behind the coastline located to the geographic east of the beach, as shown on the right image of Figure 25. While the collision regime dominates the other three simulations.

For the specific area that was simulated, all results consistently exhibit offshore transport at approximately the same location with variations in magnitude at approximately (41.36, -71.61). This variation in magnitude is attributed to the storm's intensity differences. This highlights that sediment transport is primarily wave-driven in the study area. While the primary mode of sediment transport is offshore, sediment is predominantly transported around the headlands area, particularly at the top and bottom of the domain. This raises concerns, considering that Rhode Island lacks major rivers as a sediment source. This suggests that additional sediment supply from offshore sediment sources will be necessary for beach replenishment. The offshore sediment supply needed for Green Hill Beach and Scarborough State Beach is approximately 1.3 million cubic meters, as indicated in the study by (King et al., 2016).

As for sediment grain size on the southern coast of Rhode Island, only one sediment grain size data was available for the model input. There is a variation in

sediment grain sizes along the southern shore of Rhode Island, but additional data is needed to quantify this variation. A qualitative analysis of grain size variation was conducted across different beach areas by Whaling et al. (2023). The beach composition of the west of Moonstone Beach (RI6) is 80% gravel and cobbles. The average grain size of the gravel is 1.5 cm, and the cobbles can be as large as 15 cm. In contrast, on the eastern side of Moonstone Beach, the distribution of gravel decreases to approximately 24%. Meanwhile, Charleston Beach (RI5) stands out as a predominantly sandy shoreline with only minor occurrences of gravel. Sediment grain sizes from Point Judith (RI7) are expected to be more extensive as it is known to be a rocky shoreline. Further study could incorporate different grain sizes in each RI location for a more accurate result.

It is important to note that this study used one bathymetry file for all simulations. An improved simulation approach would involve using bathymetry immediately preceding each storm impact for more accurate results. However, the primary objective of this study is not to simulate beach morphology changes following each event. Instead, the focus is on investigating variations in sediment transport trends during each storm. The total erosion and deposition were not calculated as it does not provide a comprehensive view of the spatial distribution and direction of the sediment transport (ie. Two simulations could have the same amount of erosion and deposition, but sediment could be transported in many different directions). Therefore, the simulations results are shown qualitatively.

3.5. XBeach Simulations Conclusion

Hurricane Irene, Hurricane Sandy, and the nor'easter of spring 2013 reveal consistent sediment deposition east of Green Hill Beach. Unlike the other simulations, the Hurricane Sandy simulation reveals no sediment deposition towards the west along the coastline. The source of this variation is attributed to the storm surge, which is evident in the sediment deposition occurring inland on the east and west sides of the shoreline by the top and bottom of the domain. The inland sediment deposit results from the overwash regime triggered by the storm surge level. In all four simulations, the consistent trend indicates that the wave climates and storm surges predominantly influence sediment transport. These factors stand out as the sole inputs that vary across all simulations. Seasonal variability was investigated. Minor seasonal variability was also observed from Hurricane Irene (summer) and the 2013 nor'easter (spring) simulations, which exhibit similar trends in sediment transport patterns for winter and summer storms with different intensities. Overall, there is minor seasonal variation across two simulations, Hurricane Irene and nor'easter 2013. All four simulations indicate that waves and tides primarily drive sediment transport in this area.

4. Chapter IV. Analysis of Other Available Wave and Morphological Data

4.1. Introduction

In Chapter III. XBeach simulation only covers one area of RI5: Green Hill (See Figure 2). NACCS and the GSO beach profile will be used to further investigate the variations in forcing across the southern shore of Rhode Island. This approach further quantifies the significance of spatial variability. The variation of forcing will be examined by analyzing significant wave height and water level data from various return period storm events. Storms with different return periods will be gathered from NACCS save points along the southern shore of Rhode Island. The GSO beach profile will be used to examine the variability in beach profiles. The study will also incorporate wave and wind direction data from 2011 to 2013 from WIS.

NACCS was built to improve the understanding of evolving flood risks linked to climate change within local communities (Cialone et al., 2015). NACCS used 1050 synthetic tropical storms and 100 historical extratropical events to calculate various return periods in wave height. GSO and the College of Environmental and Life Science (CELS) have collected beach profile data since 1962 (Boothroyd et al., 1988).

4.2. Methods

4.2.1. NACCS Data Retrieval

NACCS data can be accessed through a portal by NROC[14] at different save points. Save points are data handling locations that consist of 18,000 archived information on significant wave height and water level for NACCS simulated storms. Figure 26 shows the approximate save points locations and ID used in this study.

Figure 26. NACCS's station used in this study.

Data from the NACCS synthetic storm 457 was employed to evaluate the wave climate along the southern shore of Rhode Island. Storm 457 was chosen due to the track passing by Rhode Island perpendicularly, as seen in Figure 27. Furthermore, this storm represents the most severe condition, with tide water levels and significant wave heights greater than storms with a 500-year return period. The snapshot of data extrapolated from storm 457 for station ID 8401 (see Figure 26 for locations) is shown in Figure 28.

[14] https://northeastoceandata.org/data-explorer/

NACCS also provided extreme wave height and water level analysis corresponding to return periods of 10, 20, 50, 100, and 500 years. Various save points were chosen along the southern shore of Rhode Island, including two different save points in RI2: Misquamicut and RI4: East Beach 1 (see Figure 26 for save points location).

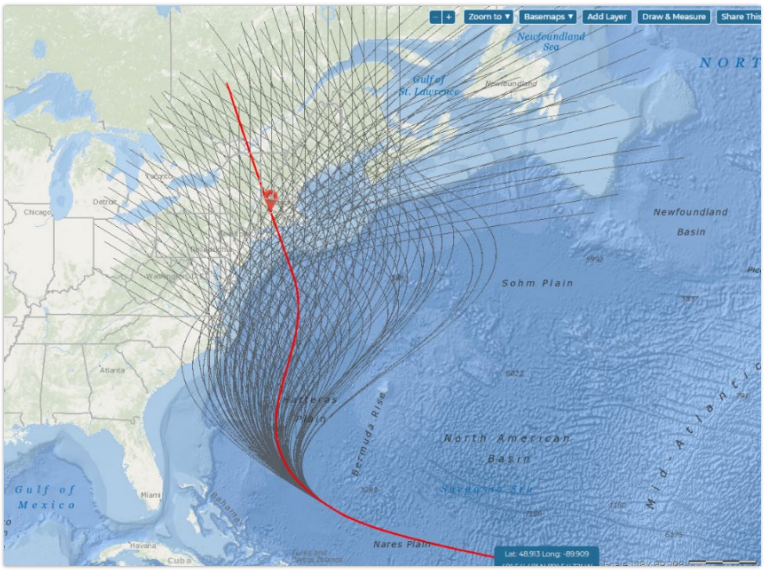

Figure 27. Track of Tropical Storm 457[15]

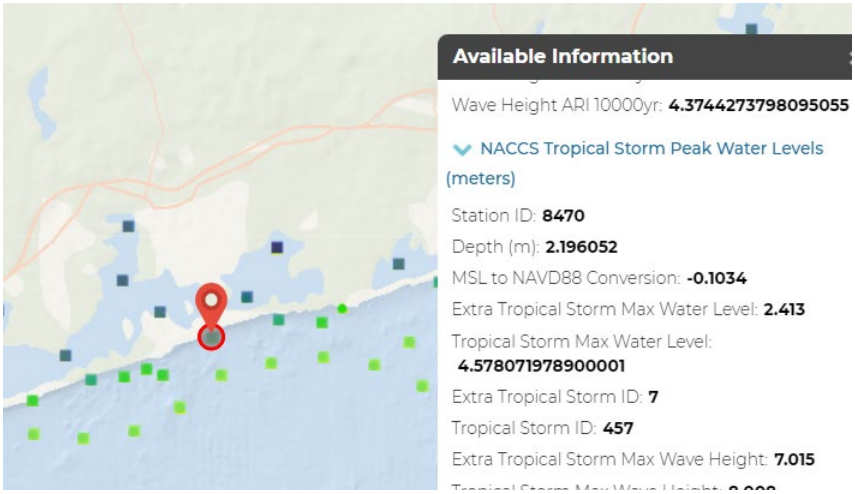

Figure 28. Snapshot of storm 457 maximum water level of 4.58 m and maximum significant wave height 8 m at RI:5 Green Hill Beach[15].

[15] https://northeastoceandata.org/data-explorer/

4.2.2. GSO Beach Profile Data and WIS data

GSO beach profiles were used to calculate the beach profile and the dune crest. Average beach data from 2012-2017 was used to analyze variations in beach profile along the coast of Rhode Island. This period also corresponds with Hurricane Sandy, Hurricane Irena, and the nor'easter of 2013, the previously used storms in XBeach. Data before 2012 was not considered since elevation was changed on the check-in survey monument. Figure 29 shows the approximate location of the beach profile while Figure 29 shows the plot of the profiles data from 2012-2017.

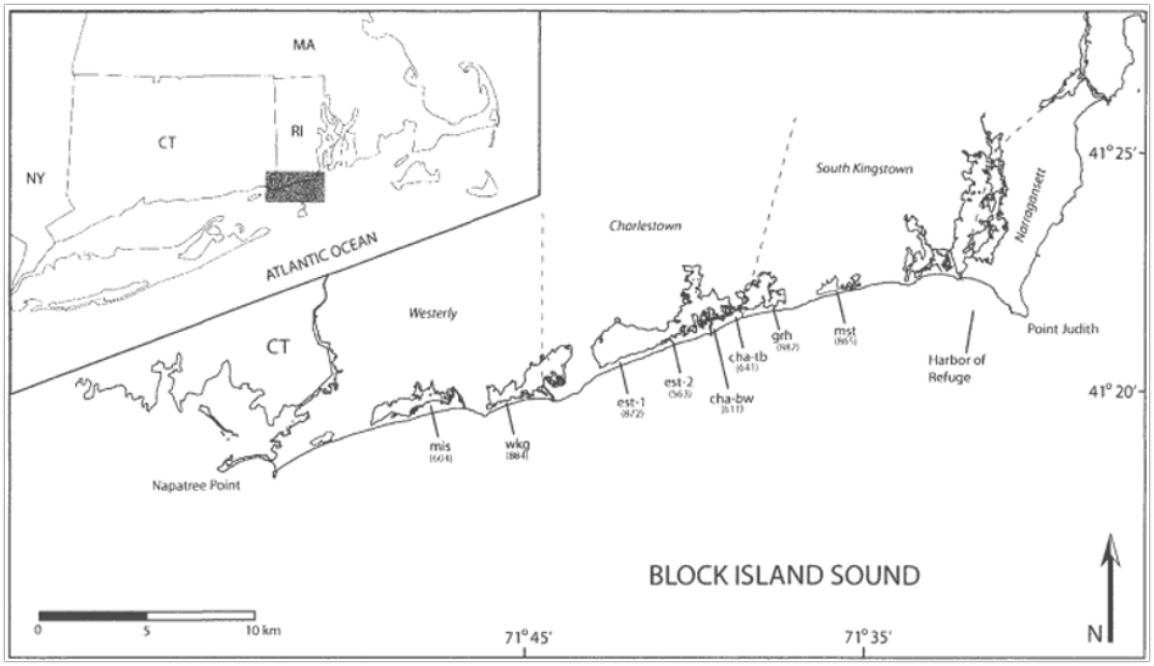

Figure 29. Approximate location of beach profile (Vinhateiro et al., 2012).

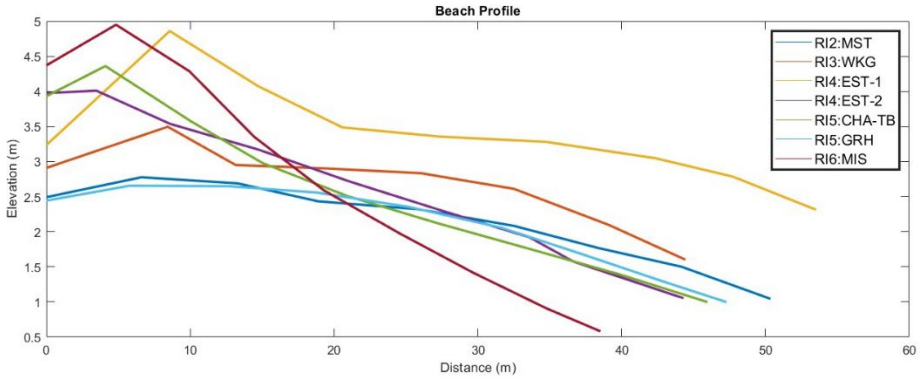

Figure 30. The profile views of average beach data from the GSO beach profile between 2012-2017 (Boothroyd et al., 1988).

Given that wave climates significantly influence sediment transport, the WIS dataset will also be employed to analyze various wave and wind directions spanning both summer and winter months from 2011 to 2013. WIS date at station 63101 is analyzed to include extreme and average summer and winter scenarios (See Figure 5 for the WIS station location). The data is shown on wave and wind roses to visually show the trend and direction of the wave and wind climates.

4.3. Results

4.3.1. NACCS data

The result from NACCS data retrieval is shown in Figure 31 and Figure 32 for water level and significant wave height respectively. Figure 31 depicts the water level plot at each save point, incorporating extreme analyses corresponding to return periods of 10, 20, 50, 100, and 500 years, along with the water level for storm 457.

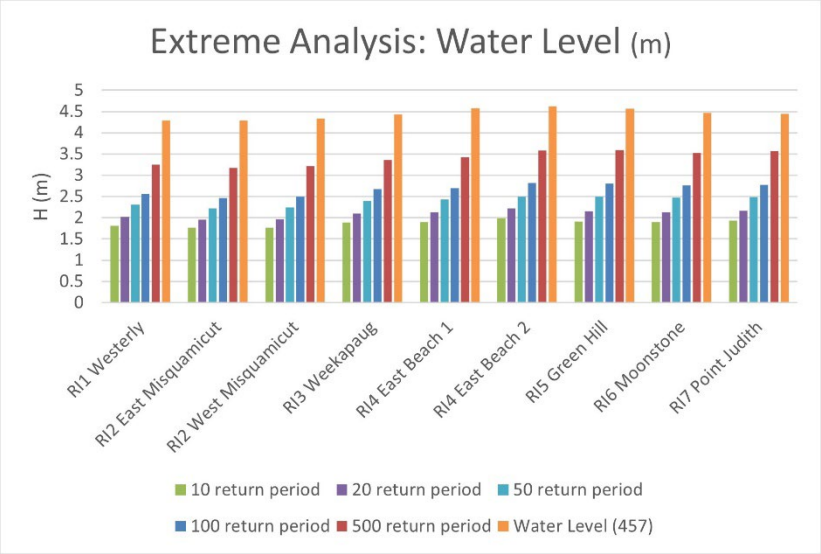

Figure 31. The water level of storm 457 (orange) compared to various return period values from NACCS (as shown in the figure above).

The water level for the 100-year return period has a mean of 2.67 m and a standard deviation of 0.135 m across all save points from RI1: Westerly to RI7: Point Judith. The mean value for storm 457 is 4.45 m, and the standard deviation is 0.126 m across. The relative standard deviation is calculated to gauge the variability relative to the mean. The relative standard deviation yields a value of 5.06% for the 100-year return period storm event, and 2.83% for storm 457, calculated from data across all save points. These findings show minor spatial variations in water levels across the southern shore,

with less than 6% variability for both cases. Similarly, Figure 32 depicts the significant wave height at each save point, incorporating extreme analyses corresponding to return periods of 10, 20, 50, 100, and 500 years, along with the data from storm 457.

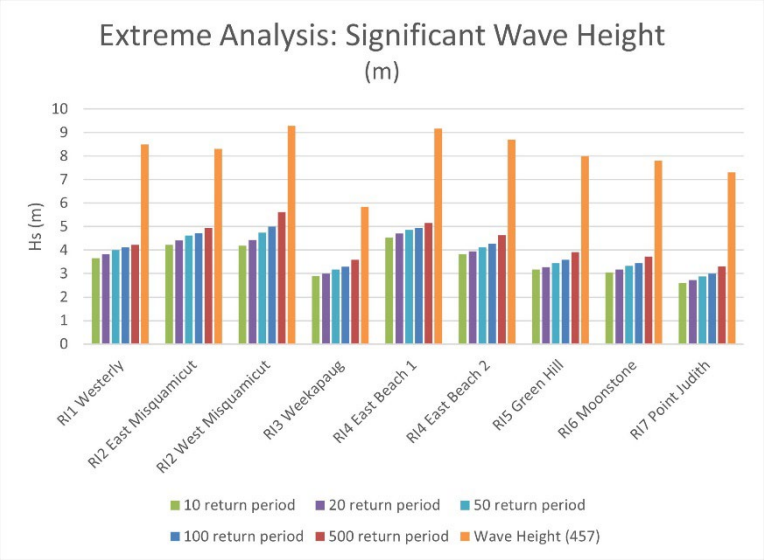

Figure 32. The significant wave height of storm 457 (orange) compared to various return period values from NACCS (as shown in the figure above).

The dataset shows spatial variability along each save point. The standard deviation for significant wave height at a 100-year return period is 0.74 m, and the mean is 4.04 m. The location with the highest significant wave height during the 100-year period is RI4: East Beach 1, with 4.99 m, while RI7: Point Judith has the lowest significant wave height, with 3.0 m. This contributes to the 49.9% difference. The relative standard deviation for the 100-year return period is 18.32% and 12.96% for storm 457 across all save points. It is important to note that the wave height for Storm 457 seems unrealistic since it exceeds that of the 500-year return period storm.

4.3.2. GSO beach profile

The results from the GSO beach profile calculation are shown in Table 3 below. The horizontal distance of the beach is defined as *H,* and the vertical elevation of the beach is defined as *V*. The beach slope is calculated by dividing vertical elevation by horizontal elevation. The dune crest is defined as the highest point of the dune on the beach profile. Values of the beach profile and the crest of the dune are shown in Table 3. The mean beach slope is 0.050, and the relative standard deviation for the beach slope is 60%. The mean of the dune crest is 5.82 m, and the relative standard deviation is 13%. There is a significant variation in beach profile along the coast of Rhode Island.

Table 3: Beach slope and dune crest summary

Profile Location	Horizontal (m)	Vertical (m)	Beach Slope. (*V*/*H*)	Dune Crest Height (m)
RI2: MST	34.15	1	0.029	6.67
RI3: WKG	48.28	1	0.020	4.86
RI4: EST-1	53.85	1	0.018	6.17
RI4: EST-2	15.22	1	0.066	5.13
RI5: GRH	22.58	1	0.044	6.88
RI5: CHA-TB	16.47	1	0.060	5.96
RI6: MIS	9.21	1	0.108	5.09

4.3.3. WIS data

Data from WIS station 63101 (See Figure 5) is plotted in wave roses on Figure 33 and Figure 34. Figure 33 depicts wave roses illustrating wave direction during the summer months from 2011 to 2013. Figure 34 depicts wave roses illustrating wave direction during the winter months from 2011 to 2013.

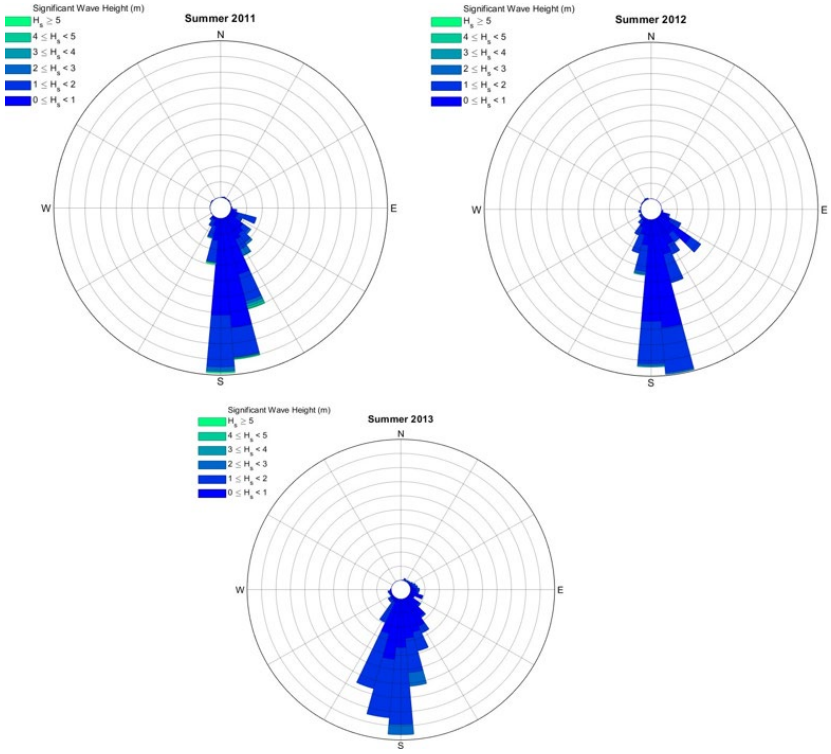

Figure 33. Wave roses from WIS station 63101 (see Figure 5) in the Summer of 2011 to 2013: 2011 (top left), 2012 (top right), and 2013 (middle).

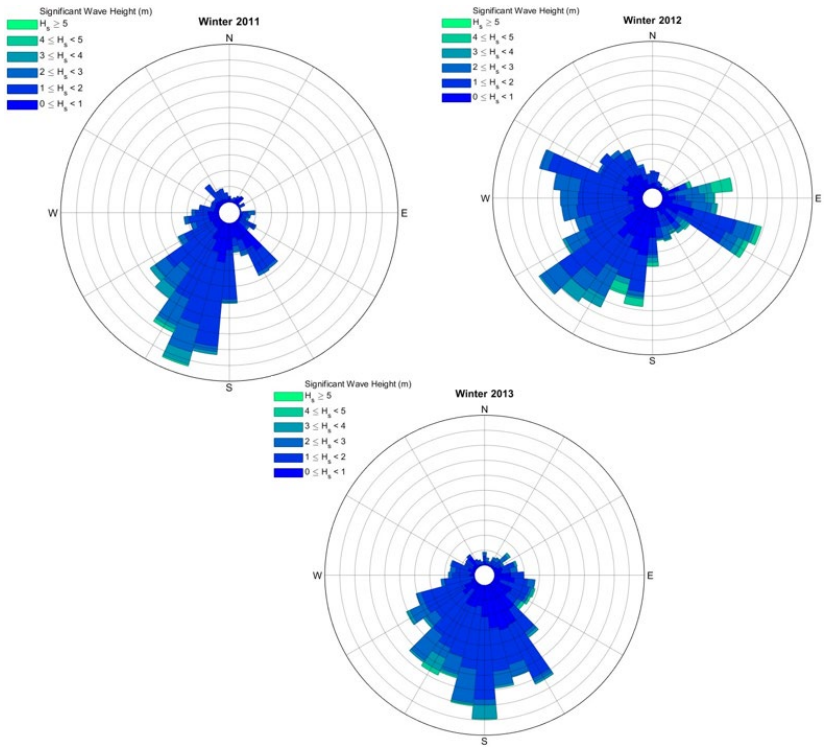

Figure 34. Wave roses from WIS station 63101 (see Figure 5) in the Winter of 2011 to 2013: 2011 (top left), 2012 (top right), and 2013 (middle).

Wave roses for the summer months between 2011 and 2013 reveal consistent dominant wave direction with minimal variability across the years. In contrast, winter months show a range of dominant wave direction from the south in 2013, and southwest in 2011 and 2013. The wind direction during the summer and winter months from 2011 to 2013 is shown in Figure 35 and Figure 36 respectively.

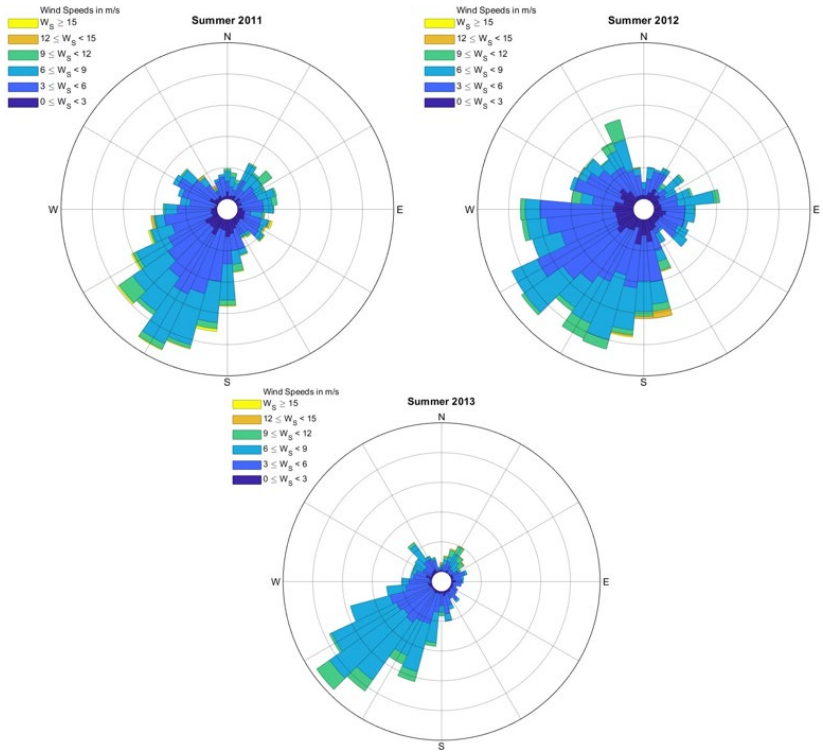

Figure 35. Wind roses from WIS station 63101 (see Figure 5) in the Summer of 2011 to 2013: 2011 (top left), 2012 (top right), and 2013 (middle).

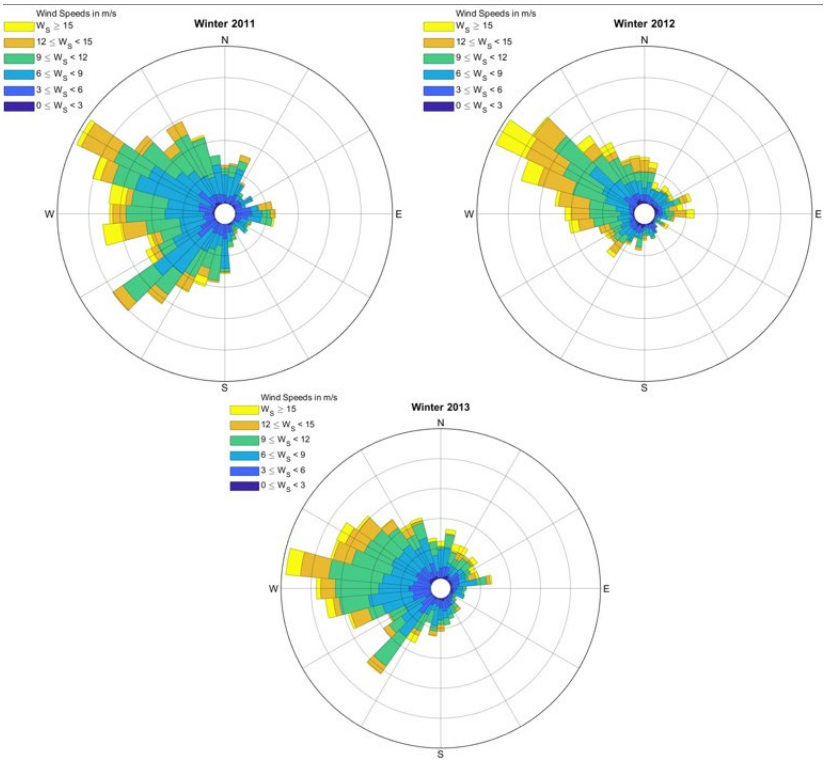

Figure 36. Wind roses from WIS station 63101 (see Figure 5) in the Winter of 2011 to 2013: 2011 (top left), 2012 (top right), and 2013 (middle).

The winter and summer wind roses from 2011 to 2013 show more variation than the wave roses. The variation is both in direction and magnitude. Summer wind roses show that wind is predominantly in the southwest direction, between 180 to 240 degrees, with a magnitude of less than 15 m/s. In contrast, the winter wind roses show that wind predominantly comes from the northwest direction between 270 to 300 degrees with a magnitude greater than 15 m/s.

4.4. Discussion

The NACCS dataset illustrates minor spatial variability along the southern shore of Rhode Island. For the 100-year return period, the significant wave height exhibits a mean of 4.04 m and a standard deviation of 0.74 m based on data across all save points. In comparison, the water level for the same return period has a standard deviation of 0.13 m and a mean of 2.67 m. RI4: East Beach 1 stands out as the location with the highest significant wave height during the 100-year period, at 4.99 m, while RI7: Point Judith has the lowest with 3.0 m (See Figure 2 for locations of RI4 and RI7). This difference is potentially due to the breakwater off of RI7: Point Judith. The relative standard deviation across all save points is 2.83% for the significant wave height and 18.3% for the water level during the 100-year return period.

The mean beach slope is 0.050, with a relative standard deviation of 60%. The dune crest displays a significantly lower mean of 5.82 m, and a relative standard deviation of 13% compared to the mean slope of the beach. This indicates a notable variation in beach profile along the coast of Rhode Island.

As for the summer and winter wave roses from 2011 to 2013, the predominant wave direction, ranging from 84.88 to 95.49 degrees, indicates a prevailing southerly wave pattern. Conversely, wave directions exhibit a broader range from 63.31 to 158.49 degrees during winter. While the wind roses from 2011 to 2013 also show variation between the summer and winter seasons. However, there is a consistent trend with the month over the years. During summer, the wind predominantly blows from the southwest, between 180 and 240 degrees, with speeds of less than 15 m/s. The winter

wind roses indicate that the wind mainly comes from the northwest, between 270 and 300 degrees, with speeds exceeding 15 m/s. In contrast, the wave roses show a consistent trend in the dominant wave direction in the summer but not the winter.

4.5. Conclusion

NACCS data suggest that spatial variations are more significant in the wave height than the water levels along the southern shore of Rhode Island, with a mean of 4.04 m compared to 2.67 m and a relative standard deviation of 18.3% compared to 2.83%. GSO beach profile data shows more significant variation in the beach slope compared to the peak dune crest, with a relative standard deviation of 60% compared to 13% of the peak dune crest. The WIS data indicates minor variability during the summer months but significant variation during winter, revealing a seasonal difference in wave direction. As for the wind roses, there is variation between the summer and winter wind direction and magnitude. However, there is a small variation between 2011 and 2013 within the same season, with the dominant wind direction from southwest in the summer and northwest in the winter.

5. Chapter V. Concluding Remarks

In conclusion, the study of spatial and temporal variability of sediment transport in the southern Rhode Island area provided some insights, as presented here. This study employed numerical models, specifically XBeach and SWAN, to simulate sediment transport and wave propagation, respectively. The simulations included four storms: Hurricane Irene, Hurricane Sandy, and nor'easter in the Fall of 2012 and Spring of 2013.

This study conducted simulations using two domains of SWAN. One domain was non-stationary, covering the North Atlantic, while the other was a stationary child domain focused on Rhode Island. The non-stationary SWAN simulations, which were used as parent grid, revealed relatively minor spatial variability in significant wave height along the boundary of the child domain or nested grid, with a mean of 7.32 m and a relative standard deviation of less than 6%. This finding shows minimal spatial variation, which supported the utilization of WIS data to force a constant boundary condition for wave simulation along the boundary of the child domain, thereby reducing computational requirements and time.

This study also shows that SWAN simulations are better aligned with the observed data from CDIP when forced with the parametric wind than the ECMWF wind because ECMWF cannot properly simulate the hurricane's core near its eye.

A qualitative analysis of XBeach simulations indicated that there are minor seasonal variations with sediment consistently transported offshore across all four simulations with differences in magnitude along the east of the coastline approximately between -71.616 degrees to -71.605 degrees for a case study in RI:5 Green Hill (See Figure 2 for location).

The collision regime remained consistent across three simulations: Hurricane Irene and nor'easter in the Spring of 2012 and 2013. The Hurricane Sandy simulation is the only simulation dominated by the overwash regime on the east and west sides near the headlands, as sediment is seen to be transported inland into the pond. The simulation also exhibited the highest sediment transport both offshore and inland, as sediment is shown to be trapped within the two headlands on either side of the domain in the Hurricane Sandy simulation. These simulations also show a small amount of sediment supply from offshore around the headland area on the east side of the domain at approximately 41.36, -71.610 degrees. It is important to consider sediment sources since there is no sediment supply from the rivers.

The NACCS datasets show spatial variations in both wave height and water levels along the southern shore of Rhode Island. The mean water level of the 100-year return period is 2.67 m with a relative standard deviation of 5.02%, while the mean significant wave height is 4.04 m with a relative standard deviation of 18.3%. These findings suggest spatial variations are more pronounced in wave height than water levels. Furthermore, the GSO beach profile data shows a mean beach slope of 0.050 and a relative standard deviation of 60%. The mean of the peak dune crest is 5.82 m and has a significantly lower relative standard deviation of 13%. This highlights considerable spatial variation in beach profile and significant wave height along Rhode Island's coastline.

In contrast, wave roses spanning the summer months from 2011 to 2013 consistently display a dominant wave direction with little variability throughout the years, ranging between 85 and 95 degrees. This indicates a prevailing southerly wave pattern during the summer seasons. Meanwhile, the winter months exhibit a wider range of wave directions,

spanning from 63 to 158 degrees, highlighting the seasonal difference in wave direction. The wind roses also show seasonal variation in wind direction and magnitude between summer and winter. However, from 2011 to 2013, there is little variation within the same season, with the dominant wind direction being from the southwest in summer and from the northwest in winter.

The limited available data on sediment grain sizes emphasizes the need for additional research to accurately quantify variations along the southern shore of Rhode Island. Qualitative analysis shows differences in sediment composition across various beach areas, emphasizing the potential significance of sediment grain size in sediment transport dynamics (Whaling et al., 2023).

In the end, this research contributes to a better understanding of sediment transport patterns in the southern Rhode Island area. The findings can inform future coastal management strategies, including beach replenishment efforts and considering various factors influencing sediment transport dynamics. Further studies incorporating additional data on sediment grain sizes and other relevant parameters will enhance the accuracy and applicability of sediment transport models in the region. Relevant parameters such as LiDAR and bathymetric data can be improved by collecting the data before, during, and after storms. This data will enhance the model simulation and help better understand sediment transport in extreme conditions.

Bibliography

Adams, P., Douglas I. L., and Lovering, J. L., "Effects of climxate change and wave direction on longshore sediment transport patterns in Southern California." Climatic Change 109: 211-228. 2011.

Amante, O., Gunn, P., Pisapio, L., and Story, M., "Mitigating coastal erosion along the Rhode Island South Shore: A Focus on Green Hill Beach." Senior Capstone Report. 2020.

Athanasiou, P., Dongeren, A., Giardino, A., Vousdoukas, M., Ranasinghe, R., and Kwadijk, J., "Uncertainties in projections of sandy beach erosion due to sea level rise: An analysis at the European scale." Scientific reports 10, no. 1:11895. 2020.

Blake, E. S., Kimberlain, T. B., Berg., R. J., Cangialosi, J. P., and Beven, J. L., "Tropical cyclone report Hurricane Sandy (AL182012) 22–29 October 2012. National Hurricane Center.", P. 157. 2013.

Booij, N., Ris, R., Holthuijsen, L., "A third-generation wave model for coastal regions." 1. Model description and validation. J Geophys Res 104(C4):7649–7666. 1999.

Boothroyd, Jon C., Nancy E. Friedrich, and Stephen R. McGinn. "Geology of microtidal coastal lagoons: Rhode Island." Marine Geology 63, no. 1-4: 35-76. 1985.

Boothroyd, J. C., R. J. Hollis, B. A. Oakley, and R. E. Henderson. "Shoreline Change from 1939–2014, Washington County, Rhode Island. 1: 2,000 scale." Rhode Island Geological Survey 45. 2016.

Boothroyd, Jon C., Scot M. Graves, & Christopher W. Galagan., "The Rhode Island

Long-Term Beach Profile Network: 1986-1988 Data (Technical Report No. 8–SRG).”1988.

Cadone, V.J., Cox, A. T., Greenwood, J.A., and Thomson, E.F., “Upgrade of tropical cyclone surface wind field model.” USACE, US Army Corps Eng, 94, 1-27. 1994.

Cavaleri, L. and Rizzoli, P.M., “Wind wave prediction in shallow water: Theory and applications.” Journal of Geophysical Research: Oceans, 86(C11), pp.10961-10973. 1981.

Chai, T., and Draxler, R., “Root mean square error (RMSE) or mean absolute error (MAE).” Geoscientific model development discussions 7, no. 1:1525-1534. 2014.

CERC., Shore Protection Manual; “US Army Corps of Engineers – Washington, DC. U.S. Government PrintingODce,” Vicksburg, https://doi.org/10.5962/bhl.title.47829. 1984.

Chandramohan, P., and B. U. Nayak. “Longshore sediment transport model for the Indian west coast.” Journal of coastal research: 775-787. 1992.

Cialone, Mary A., T. Chris Massey, Mary E. Anderson, Alison S. Grzegorzewski, Robert D. Jensen, Alan Cialone, David J. Mark et al. “North Atlantic Coast Comprehensive Study (NACCS) coastal storm model simulations: Waves and water levels. US Army Engineer Research and Development Center, Coastal and Hydraulics Laboratory,” 2015.

D’Alessandro, F., Giuseppe Roberto Tomasicchio, Ferdinando Frega, Elisa Leone, Antonio Francone, Daniela Pantusa, Giuseppe Barbaro, and Giandomenico Foti. “Beach–Dune System Morphodynamics.” Journal of Marine Science and Engineering 10, no. 5: 627. 2022.

Dail, Holly J., Mark A. Merrifield, and Mike Bevis. “Steep beach morphology changes due to energetic wave forcing.” Marine Geology 162, no. 2-4: 443-458. 2000.

Davis Jr, Richard A., and Miles O. Hayes. “What is a wave-dominated coast?.” In Developments in Sedimentology, vol. 39, pp. 313-329. Elsevier, 1984.

Dee, Dick P., S. M Uppala, Adrian J. Simmons, Paul Berrisford, Paul Poli, Shinya Kobayashi, U. Andrae et al. “The ERA-Interim reanalysis: Configuration and performance of the data assimilation system.” Quarterly Journal of the Royal Meteorological Society 137, no. 656: 553-597. 2011.

González-Santamaría, Raúl, Qingping Zou, and Shunqi Pan. “Modelling of the impact of a wave farm on nearshore sediment transport.” In 33rd International Conference on Coastal Engineering 2012. Coastal Engineering Research Council, 2012.

Hashemi, M. R., Kresning, B. Hashemi, J. and Ginis, I. “Assessment of hurricane generated loads on offshore wind farms; a closer look at most extreme historical hurricanes in New England.” Renewable Energy 175: 593-609. 2021.

Hayward, S., Hashemi, M. R., Torres, M., Grilli, A., Grilli, S., King, J., Baxter, C., And Spaulding, M., “Numerical simulation of coastal erosion and its mitigation by living shoreline methods: A case study in southern Rhode Island.” Shore & Beach 86, no. 4 P.13. 2018.

King, J., Boothroyd, J. and Fugate, G., “Estimating Necessary Volumes of Sand Beach Replenishment Along the Rhode Island South Shore: Data from the Rhode Island Shoreline Change Special Area Management Plan (“BeachSAMP”), Deliverable E: FINAL FINDINGS REPORT.” Coastal Resources Management

Council, University of Rhode Island, and Bureau of Ocean Energy Management. 2016.

Komen, G.J., S. Hasselmann, and K. Hasselmann, “On the existence of a fully developed wind-sea spectrum, J. Phys. Oceanogr.” 14, 1271-1285. 1984.

Leone, A. J., Grilli, A., Grilli, S., Walsh, J., Baxter, C., DeBoef, B., “Predicting Morphodynamic Long-Term Changes Along the Southern Rhode Island Shoreline in the Next Decades.” Master’s Thesis, ProQuest Dissertations and Thesis Database, University of Rhode Island, 2022.

Luijendijk, Arjen, Gerben Hagenaars, Roshanka Ranasinghe, Fedor Baart, Gennadii Donchyts, and Stefan Aarninkhof. “The state of the world’s beaches.” Scientific reports 8, no. 1 P.6641. 2018.

Mayer, Larry, Martin Jakobsson, Graham Allen, Boris Dorschel, Robin Falconer, Vicki Ferrini, Geoffroy Lamarche, Helen Snaith, and Pauline Weatherall. “The Nippon Foundation—GEBCO seabed 2030 project: The quest to see the world’s oceans completely mapped by 2030.” Geosciences 8, no. 2. P. 63. 2018.

National Geophysical Data Center, NOAA. doi:10.7289/V5MS3QNZ https://www.ncei.gov/products/coastal-relief-model. 2023.

Olfateh, M., David P. Callaghan, Peter Nielsen, and Tom E. Baldock. “Tropical cyclone wind field asymmetry—Development and evaluation of a new parametric model.” Journal of Geophysical Research: Oceans 122, no. 1. P.458-469. 2017.

Roelvink, D., van Dongeren, A., McCall, R., Hoonhout, B., van Rooijen, A., van Geer, P., de Vet, L., and Nederho↵, K. XBeach Manual. Deltares,UNESCO- IHE Institute of Water Eduation and Delft University of Technology. 2015.

Schambach, L., Grilli, A.R., Grilli, S.T., Hashemi, M.R. and King, J.W., "Assessing the impact of extreme storms on barrier beaches along the Atlantic coastline: Application to the southern Rhode Island coast." Coastal Engineering, 133, pp.26-42. 2018.

Schambach, L., Grilli, A.R., Grilli, S.T., "A comparison of wave and erosion modeling methods for the 100-year storm in Southern Rhode Island." Master's thesis, University of Rhode Island, 2017.

Small, C., Tyler Blanpied, Alicia Kauffman, Conor O'Neil, Nicholas Proulx, Mathew Rajacich, Hailey Simpson et al. "Assessment of damage and adaptation strategies for structures and infrastructure from storm surge and sea level rise for a coastal community in Rhode Island, United States." Journal of Marine Science and Engineering 4, no. 4, P.67. 2015.

Slott, Jordan M., A. Brad Murray, Andrew D. Ashton, and Thomas J. Crowley. "Coastline responses to changing storm patterns." Geophysical Research Letters 33, no. 18. 2006.

Sarpkaya, Turgut, Michael Isaacson, and J. V. Wehausen. "Mechanics of wave forces on offshore structures." Journal of Applied Mechanics. P.466-467. 1982.

Shetty, A., and Jayappa, K. S., "Seasonal variation in longshore sediment transport rate and its impact on sediment budget along the wave-dominated Karnataka coast, India." Journal of Earth System Science. 129: 1-14. 2020.

Skadden, J. E., Hashemi, M. R., Grilli, A., King, J., Oakley, B., "Numerical Simulation of Coastal Erosion and Recovery During and Following Storm Events." Master's Thesis, ProQuest Dissertations and Thesis Database. University of Rhode Island., 2021.

Toimil, A., Losada, I. J., Camus, P. and Díaz-Simal, P., “Managing coastal erosion under climate change at the regional scale.” Coastal Engineering", 128, pp.106-122. 2017.

USACE (US Army Corps of Engineers). “Coastal engineering manual. Engineer manual 1110-2-1100.” 2002.

Vinhateiro, N.D., 2012. “Mechanisms of shoreline change on the Rhode Island South Coast: Past, present, and future.” Doctoral Dissertation, ProQuest Dissertations and Thesis Database. University of Rhode Island, 2017.

Whaling, I. C., Walsh, J.P., Ginnis, I., Parent, J., Conery, I., “Evolution of Coastal Barrier Systems in Southwestern Rhode Island in Response to Storms and Anthropogenic Forcing.” Master’s Thesis, ProQuest Dissertations and Thesis Database, University of Rhode Island, 2023.

Whitham, G.B., “Linear and nonlinear waves.” Wiley, New York, 1974.

Woods Hole Sea Grant Program. “Longshore Sediment Transport.” Cape Cod, Massachusetts. Cape Cod Cooperative Extension. P 2-7. https://www.capecod.gov/wp-content/uploads/2022/03/LST.pdf, April 2021.

Woods Hole Group. “Wave, tide and current data collection contract no. W912WJ-09-D-0001-0026.” 2012.

Walsh, K., “Objective detection of tropical cyclones in high-resolution analyses.” Monthly Weather Review 125, no. 8: 1767-1779, 1997.

Wu, J., “Wind-stress coefficients over sea surface from breeze to hurricane.” Journal of Geophysical Research: Oceans, 87(C12), 1982.